2017

Effects of tauopathy on the morphological properties of fan and stellate cells in the entorhinal cortex of the P301S mutant mouse model

BOSTON UNIVERSITY

SCHOOL OF MEDICINE

Thesis

EFFECTS OF TAUOPATHY ON THE MORPHOLOGICAL PROPERTIES OF FAN AND STELLATE CELLS IN THE ENTORHINAL CORTEX OF THE P301S MUTANT MOUSE MODEL

by

MICHAEL FOWLER

B.S., Marquette University, 2011

Submitted in partial fulfillment of the

requirements for the degree of

Master of Science

2017

Approved by

First Reader _____

Jennifer Luebke, Ph.D.
Professor of Anatomy and Neurobiology

Second Reader _____

Matthew D. Layne, Ph.D.
Associate Professor of Biochemistry

ACKNOWLEDGMENTS

I would like to thank my family, my mentors Dr. Luebke, Dr. Medalla, and Dr. Layne, and all of the friends I have made over the past two years, both from the Luebke lab as well as the classmates in my program. The support and friendships I have made is more valuable than any degree I could be awarded. I am truly blessed to have met each and every one of these individuals, and I know that they have helped me become a better individual.

EFFECTS OF TAUOPATHY ON THE MORPHOLOGICAL PROPERTIES OF FAN AND STELLATE CELLS IN THE ENTORHINAL CORTEX OF THE P301S MUTANT MOUSE MODEL

MICHAEL FOWLER

ABSTRACT

Neurodegenerative diseases generally correlate with age; as the US population's average age increases, neurodegenerative ailments will contribute a greater burden on the health care system. One of the most prevalent, Alzheimer's disease, is known to associate with tau proteins with evidence suggestive that abnormal function may initiate neurodegeneration. The entorhinal cortex is one of the earliest regions found to exhibit neuronal atrophy in Alzheimer's disease. This study analyzed two major neuron types in the entorhinal cortex, fan cells and stellate cells, using the P301S mouse model for tauopathy. Laser-scanning confocal microscopy and software were used to reconstruct and analyze dendrite morphology between the two neuron types. Our results found that stellate cells of transgenic mice exhibited dendritic atrophy, with decreases in morphological parameters such as dendritic length, dendritic complexity, and number of primary dendrites in comparison to wild-type stellate cells. On the other hand, fan cells of transgenic mice did not show decreases in these parameters. Instead, fan cells of transgenic mice showed increases in surface area and volume in a convex hull model, as well as an increase in total Sholl radius from soma in comparison to wild type fan cells. These results suggest that neurons may respond differently to tauopathic stress. Additionally, noting distinct morphological differences between wild type fan cells and

stellate cells, such as stellate cells having greater spine density and basal dendritic extensions, our data hints that morphological characteristics may predict susceptibility to pathogenic effects of tau.

TABLE OF CONTENTS

LIST OF TABLES

LIST OF FIGURES

LIST OF ABBREVIATIONS

AD ..... Alzheimer's Disease

AMPA ..... α-Amino-3-hydroxy-5-metthyl-4-isoxazolepropionic acid

AMPAR ..... α-Amino-3-hydroxy-5-metthyl-4-isoxazolepropionic acid receptor

AP .....Action potential

CamkII ..... Calmodulin-dependent kinase II

COX-2 .....Cyclooxygenase-2

Eif2α..... α subunit of eukaryotic translation initiation factor 2

EC .....Entorhinal cortex

FC .....Fan cell

FTDP-17 .....Frontotemporal dementia with parkinsonism-17

G3BP .....Ras GTPase-activating protein-binding protein

GABA ..... γ- aminobutyric acid

HDAC .....Histone Deacetylase Inhibitor

htau.....Human tau

LEC ..... Lateral entorhinal cortex

MAPT .....Microtubule-associated protein tau

MARCKS.....Myristoylated Alanine Rich Protein Kinase C Substrate

MEC ..... Medial Entorhinal Cortex

MCI ..... Mild cognitive impairment

NADH .....Nicotinamide adenine dinucleotide

NFT .....Neurofibrillary tangle

NMDA ..... N-methyl-D-aspartate

PBS ..... Phosphate buffered saline

PERK ..... RNA-like endoplasmic reticulum kinase

PKC ..... Protein kinase C

PSD-95 ..... Postsynaptic density protein 95

RBP ..... mRNA binding protein

SC ..... Stellate cell

SG ..... Stress granule

SIRT1 ..... Sirtuin 1

TDP-43 ..... TAR DNA-binding protein 43

TIA-1 ..... T-cell intracytoplasmic antigen 1

TNF-α ..... Tumor necrosis factor α

TTP ..... Tristetraprolin

WT ..... Wild-type

INTRODUCTION

Overview of Neurodegenerative Diseases

Neurodegenerative diseases in a general sense are ailments that cause nervous tissue to degrade, specifically by causing the debilitation and death of neurons. As neurons are incapable of replication beyond early development and generally are not able to be replaced, damage from neurodegenerative diseases is typically irreversible. Examples of neurodegenerative diseases include Alzheimer's Disease (AD), Parkinson's disease, and Huntington's disease.

Overall, the incidence as well as severity of neurodegenerative diseases such as AD have been found to be correlated with age (Hebert et al. 2003). Because of the expected rise in age of the United States' population (Anderson et al. 2012), overall healthcare costs for neurodegenerative diseases is expected to increase (Geldmacher, 2012). For example, over the next 50 years, the prevalence of AD is expected to increase by a factor of three in the US population; additionally, the number of persons aged 85 or more will be expected to quadruple by this same time frame (Hebert et al. 2003). Ailments like AD can be expensive to manage as most individuals require full-time care, with Geldmacher, 2002 noting that dementia caused from AD results in the third most costly illness in the United States. Additionally, many neurodegenerative diseases can have a relatively lengthy duration creating a scenario that can strongly burden the public healthcare infrastructure (Dharmarajan and Gunturu, 2009). Beyond financial costs though, the toll that neurodegenerative diseases can take on the sufferer are immense: one survey of caregivers found that patients exhibited anxiety (63.4%), depression (63.4%),

hopelessness (35.2%), feelings of worthlessness (29.7%), and tearfulness (27.1%) (Schulz et al. 2008). Caregivers themselves also showed moderate levels of depressive symptoms (Schulz et al. 2008).

Tauopathies are a subset of neurodegenerative disease in which the primary pathology of the disease is caused by misfolding or hyperphosphorylation of the protein tau (Lee and Leugers, 2012). The earliest and most prevalent symptom that individuals with neurodegenerative diseases related to tauopathies suffer from is increasing memory loss (Meier et al. 2016). Symptoms can range, however, from dementia to movement disorders (Xu et al. 2014). While studying the effects of tauopathy on the hippocampus in the P301S mouse model—a genotype for frontotemporal dementia with parkinsonism linked to chromosome 17 (FTDP-17), useful in repeating human symptoms of tauopathy (Takeuchi et al. 2011)—Xu et al. 2014 noted that visuospatial memory skills deteriorated first; this was then followed by a lack of exploring activity and finally locomotor dysfunction. During the period where only visuospatial memory skills had deteriorated, only soluble tau was found present in neurons, with no neuron cell loss being observed at this point (Xu et al. 2014). This differed later in the course of the disease when locomotor dysfunction was noted: at this point, insoluble tau was observed in addition to soluble forms (Xu et al. 2014).

One challenge with neurodegenerative disorders is that they can be difficult to diagnose as symptoms may overlap with other ailments (Gómez-Río et al. 2016). Additionally, damage may occur to nervous tissue before symptoms become noticeable. For example, in AD, full clinical symptoms do not develop until after pathological effects

in the brain, such as neuronal atrophy, have already taken place (deToldeo-Morrell et al. 2007). In many cases, early symptoms of AD are identical to other ailments, making diagnosis even more difficult. For example, Mild Cognitive Impairment (MCI) which is a general cognitive ailment, impairs individuals mildly enough so as to not interfere with allowing them to conduct normal activities, but cognitively impairs the individual to a greater extent when age is taken into account (Ritchie et al. 2001). Many times these symptoms overlap with mild AD, and, making the situation even more complicated, MCI is known to progress to AD in some patients (Peterson et al. 1999).

Overview of the Entorhinal Cortex

The symptoms for a specific neurodegenerative disease relates to the region of the brain being impacted. For example, in regards to AD, at the earliest stages of the disease, regions of the entorhinal cortex and hippocampal formation are impacted (deToldeo-Morrell et al. 2007). The hippocampus, an important region for assimilating information before memory formation can occur has been shown in certain tauopathies to exhibit atrophy and structural alterations, in line with many studies of tauopathies negatively impacting memory (Xu et al. 2014). For AD specifically, one of the earliest regions of the brain to be impacted is the entorhinal cortex (EC) which provides the main afferent input into the hippocampus (deToledo-Morrell et al. 2007).

Structure of the Entorhinal Cortex

The entorhinal cortex (EC) is part of a larger functional unit: the hippocampal formation, which includes the EC, dentate gyrus, hippocampus, subiculum,

presubiculum, and parasubiculum (Li and Pleasure, 2013), each of which can be visualized in three different organisms in Figure 1. In mice, the EC is located in the caudal section of the temporal lobe, unlike in primates where it is located rostrally. The EC is divided into two sections: the lateral entorhinal cortex (LEC) and the medial entorhinal cortex (MEC). From a morphological view, a major difference between the LEC and MEC is found in layer II where the MEC appears more uniform in appearance compared to the LEC which appears more heterogeneous; additionally, the MEC has a more noticeable lamina dissecans compared to the LEC (Burwell and Agster, 2008).

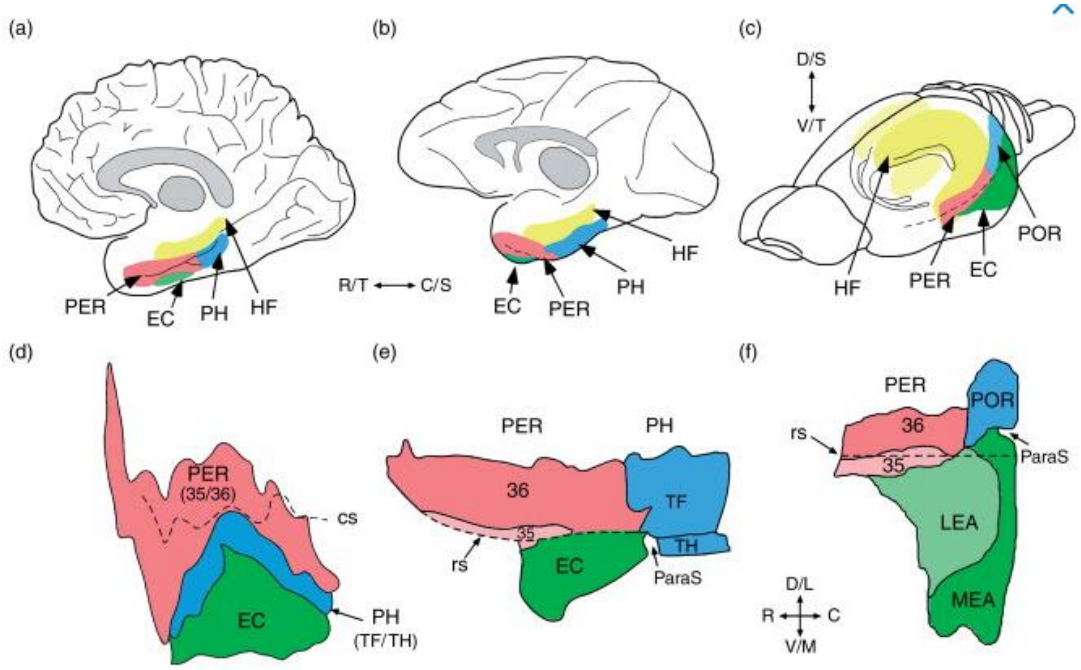

Figure 1. Location of the Entorhinal Cortex Across Three Species (Burwell and Agster, 2008). Shown are representations of the entorhinal cortex as well as surrounding regions of the human (a,d), monkey (b,e), and rodent (c,f) brain. The top panels show a lateral view of the main structures, whereas the lower panels show an unfolded view of the cortical structure. cs, collateral sulcus; EC, entorhinal cortex; HF, hippocampal formation; LEA, lateral entorhinal area; MEA, medial entorhinal area; ParaS, parasubiculum; PER, perhinal cortex; PH, parahippocampus; POR, postrhinal cortex; rs, rhinal sulcus; TF, thalamic fasciculus; TH, thalamus

Interconnectivity to Surrounding Neural Network for the Entorhinal Cortex

The EC is complex with regard to its anatomical connections (Burwell and Agster, 2008). Functionally, the EC is significant in that its axons comprise the major excitatory input to the apical dendrites of neurons in the hippocampus via the performant path, specifically regions CA1 to CA4 and the dentate gyrus (Bielle and Garel, 2013). Regarding layers, layer II neurons from the EC connect with granule cells of the dentate gyrus and CA3, while layer III neurons from the EC connect to the CA1 and subiculum

(Tahvildari and Alonso, 2005). Additionally, the EC also acts as an end point from signaling originating from the hippocampal formation (Craig and Commins, 2006). For example, the subiculum is noted to relay back to the EC, before the signaling is eventually relayed back to the cortex (Tahvildari and Alonso, 2005). Overall, the general layout of the hippocampal formation is designed such that most components, including the EC, relay their outputs to the subiculum, which subsequently connects with the neocortex (Craig and Commins, 2006).

Physiological Function and Significance of the Entorhinal Cortex

Being part of the mesial temporal lobe memory system, the EC is critical in receiving sensory information from the neocortex, and then relaying that information to the hippocampus via the performant pathway (deToledo-Morrell et al. 2007). The EC functions by relaying sensory information to different regions of the hippocampal formation; additionally, it plays a role in organizing spatial information (Burwell and Agster, 2008). The LEC is crucial in transferring information regarding distinct objects or items from the perihinal cortex to the hippocampus, while the MEC is critical in relaying both spatial and contextual information from the postrhinal cortex to the hippocampus (Agster and Burwell, 2013). Additionally, the LEC has long been known for its role of relaying olfactory information from the lateral olfactory tract to the dentate gyrus (Wilson and Steward, 1978). When this information arrives at the dentate gyrus and CA3 regions, information is then combined together to allow for both time and spatial inputs to be provided with an episodic memory (Knierim et al. 2006). Analyses in mice have shown that inactivating either the MEC or LEC will create deficiencies in episodic task

performance, but in different ways. A study by Yoo and Lee, 2017 showed that when the MEC was inactivated, mice were not capable of making decisions when provided visual signals, though inactivation of the LEC did not result in this observation. On the other hand, when a specific task was required, the LEC was shown to be vital in performing this function (Yoo and Lee, 2017). When the entire EC is impaired, as was done in a study by Parron et al. 2004, it was shown that the animal was incapable of performing visuospatial tasks when relying on distal landmarks, but was successful in completing the task if utilizing proximal landmarks. This would suggest that when processing spatial information, additional neural networks beyond the EC are employed when synthesizing visual information from other than distal landmarks (Parron et al. 2004).

Neurodegeneration in the Entorhinal Cortex

In many neurodegenerative diseases where memory function is impaired, such as AD or MCI, *post mortem* reports have shown the EC as well as the regions around the EC to have pathological properties, including atrophy via MRI analysis (deToldeo-Morrell et al. 2007). In addition to these pathological observations, the overall physical size of the EC can be a useful predictor in likelihood of conversion of MCI to AD; deToledo-Morrell et al. 2007 noted that a roughly 0.1 unit decrease in EC volume related to the doubling of odds for conversion of MCI to AD to occur. The decrease in volume and not simply neuron count suggests a decrease in neuropil and synapses (Gómez-Isla et al. 1996).

In total, roughly 7 million neurons exist in the human EC; this value remains relatively constant throughout adulthood, but is found to be reduced significantly at the

earliest stages of neurodegenerative diseases such as AD to such a great extent that neuronal loss must occur before clinical symptoms of the disease become apparent (Gómez-Isla et al. 1996). Although all layers of the EC eventually become affected, neuron loss occurs earliest and most predominantly in the superficial cortical layers of II and IV, while the deeper cortical layers (V, VI) and layers I and III only become impacted at a more advanced stage of the disease (Romito-DiGiacomo et al. 2007; Gómez-Isla et al. 1996). In addition to individuals with AD, MCI has been shown to cause significant atrophy and reduction of volume in layer II, with the degree of neuronal loss correlating to diminishment on performance of clinical tests for declarative memory (Kordower et al. 2001). When analyzing the LEC and MEC separately, studies have shown the LEC to be more vulnerable to neurodegeneration compared with the MEC, and is more likely to exhibit overall pathological features at the earliest instance of AD (Khan et al. 2014). In the study by Khan et al. 2014, it was noted that basal metabolic rates, measured by cerebral blood flow, were significantly higher in the LEC compared to other surrounding regions of the brain, including the MEC, suggestive that metabolic rates could influence vulnerability for preclinical regions where neurodegeneration begins. Of all symptoms, evidence suggests then that the earliest should derive from neurodegenerative compromise of the LEC, making the anterior pathway uniquely vulnerable for early stage effects of AD (Klein et al. 2016). As was previously mentioned, olfaction is linked to the LEC; therefore, it is of interest to note that AD-related olfactory dysfunction is an early symptom the disease (Wesson et al. 2010). Wesson et al. 2010 found that not only was there a correlation between the degree and

incidence of olfactory symptoms, but also non-fibrillar amyloidβ (Aβ) deposition, a pathogenic manifestation of AD, was found in the olfactory bulb before being detected in any other region of the brain. Additionally, there is other evidence that pathological activity in the LEC precedes the MEC. For example, the LEC was found to have a greater density of pathological amyloid plaques as well as develop the plaques earlier than the MEC (Klein et al. 2016). This suggested greater physiological disruption of the LEC as the greater density of plaques correlated with a decrease in both frequency and power of gamma oscillation measurements relative to the MEC, significant as gamma oscillations act as a gauge for measuring information transfer (Klein et al. 2016).

Cells of the Entorhinal Cortex

When comparing layer II neurons of the LEC and MEC, it was found that neurons were distinctly different in terms of morphological and electrophysiological properties (Tahvildari and Alonso, 2005). On the other hand, morphological and electrophysiological properties were found to be very similar when comparing layer III neurons of the LEC and MEC (Tahvildari and Alonso, 2005). The stellate cell (SC) was the predominant type of neuron when examining layer II of the MEC, comprising roughly 69 percent of neurons surveyed in one study (Alonso and Kirk, 1993). On the other hand, when examining layer II of the LEC, the predominant neuron was the fan cell (FC) (Tahvildari and Alonso, 2005). Both SCs and FCs were found to have a somewhat similar morphology, with both possessing several dendrites that extend through layers I and II of the EC for example (Marcantoni et al. 2014).

Major differences exist in terms of morphology between the two major cell types analyzed in this study. FCs possess multiple primary dendrites that are relatively thick and branch in both horizontal and ascending directions (Tahvildari and Alonso, 2005; Canto and Witter, 2012). This results in a shape that resembles a half-moon (or a fan) with the neuron's base parallel to layer II (Tahvildari and Alonso, 2005; Canto and Witter, 2012). It should be noted that occasionally fan cells can possess scarce dendrites in the basal orientation; this should not prevent the neuron from being classified as a fan cell (Tahvildari and Alonso, 2005) (Figure 2).

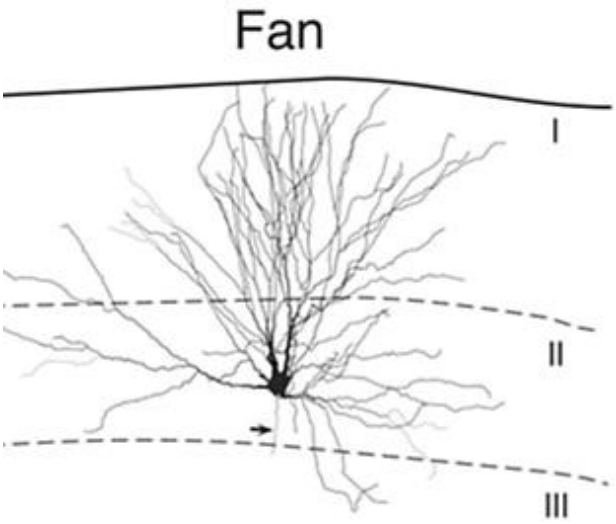

Figure 2: Pictorial representation of a fan cell (Tahvildari and Alonso, 2005). The image shows a fan cell's morphological pattern of horizontal and apical dendrites as well as its location in the entorhinal cortex (layer II). Note that for the most part the neuron does not have a basal projection of dendrites, except for the faint dendrite highlighted by the arrow. Regardless of this anomaly, totality of evidence would still require this cell to be classified as a fan cell.

The most distinctive morphological characteristic of fan cells is their relative lack of descending dendrites heading towards layer III (Tahvildari and Alonso, 2005). The fan cell's soma is polygonal in shape, and spine density amongst primary dendrites is relatively sparse (Tahvildari and Alonso, 2005; Canto and Witter, 2012). Primary dendrites for SCs, contrastingly, are equally spaced around the soma and branch extensively (Canto et al. 2008). Unlike FCs, SCs do possess basal dendrites, but they are relatively smaller compared to their apical dendrites (Canto et al. 2008). One highly characteristic feature about SCs is the strong amount of spines on their dendritic tree (Canto et al. 2008).

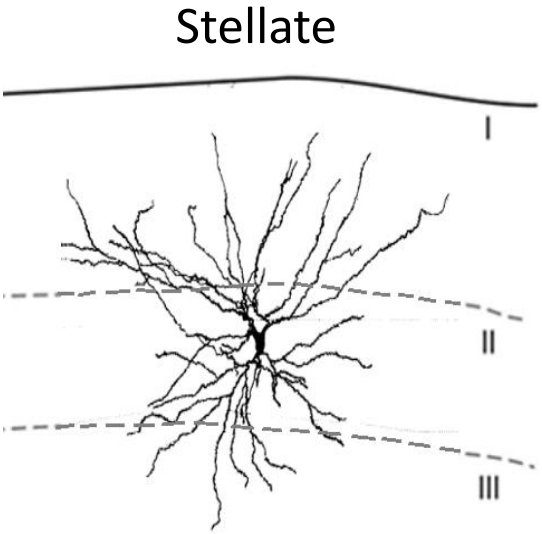

Figure 3: Pictorial representation of a stellate cell (Alonso and Kirk, 1993; Tahvildari and Alonso, 2005). The image shows a stellate cell's morphological pattern of dendrites branching in all directions, as well as its location in the entorhinal cortex (layer II). Note that unlike the fan cell, stellate cells do possess a basal projection of dendrites.

The electrophysiological properties the two cell types differ as well, with SCs firing at higher frequencies compared to FCs when injecting minimum current to generate an action potential (AP) (Marcantoni et al. 2014). Additionally, when providing maximum current, SCs were found to fire at higher rates with increased spike frequency adaptation compared to FCs (Marcantoni et al. 2014). When analyzing transgenic mice with early Aβ accumulation, SC firing rate decreased to only a minor extent; while FC AP firing rate decreased significantly, suggestive that FCs may be more prone to negative effects caused by neurodegenerative tauopathies (Marcantoni et al. 2014). Marcantoni et al. 2014 notes that because FCs provide a major role in memory acquisition by acting as a major input to the hippocampus via the performant path, the observation that these neurons seem to be heavily impacted by mutant tau corresponds to clinical symptoms seen in early AD.

Review of Spine Properties

As one of the earliest sections to develop hyperphosphorylated tau accumulations in tauopathies, understanding the functionality of spines is critical for realizing the pathogenic significance that loss of spines can play in neurodegeneration. Functionally, dendritic spines are dynamic structures, with changes in shape as well as creation and destruction being shown to be essential for long-term memory and cognition (Kasai et al. 2010). These alterations are governed by underlying actin filaments and have the capability of being morphologically altered in the timeframe of seconds (Hoffmann et al. 2013; Testa et al. 2012). Through this morphological plasticity, neurons are capable of altering their synaptic interconnections (Hoffmann et al. 2013), and disorders in this

capability have been shown to lead to dementia and cognitive impairment (Kasai et al. 2010). Larger spines may maintain old memories, while smaller spines that are newly formed appear to assist with new memories (Xu et al. 2014). Interestingly, the size or volume of the spine is proportional to both postsynaptic density and the AMPA receptor content (Hoffman et al. 2013). Spine density has also been shown to be important for cognitive ability as spine density has been shown to diminish in neurodegenerative diseases that negatively impact cognition (Xu et al. 2014). Cognitive function was able to be corrected in AD mice when spine density was increased to control, non-disease levels by removing intraneural Aβ plaques by administering HDAC inhibitor 4-phenylbutyrate, an agent which promotes protein folding thus preventing the accumulation of Aβ plaques (Ricobaraza et al. 2010).

Normal Function of Tau

Although tau protein plays an important role in many neurodegenerative ailments, it's normal role is incredibly vital to the health of a neuron, as it acts to stabilize microtubules by helping assemble tubulin monomers, critical for maintaining the shape of the neuron (Buée et al. 2000). Additionally, as microtubules are pivotal for transport of both proteins and organelles, tau has a direct impact in the neuron's capacity to perform this function (Buée et al. 2000). In total, six tau isoforms exist in homeostatic balance, all translated via alternative mRNA splicing from the MAPT gene located on chromosome 17q21.31 (Spillantini et al. 2013). Generally tau is located in the axon of neurons (Binder et al. 1985), but translocates to somatodendritic regions in pathogenic states (Xu et al. 2014).

Pathogenic Properties of Mutant Tau

Overall, 48 tau mutations have been found to be linked to tauopathies (Zhang et al. 2016; Meier et al. 2016). Although multiple mutations in the tau gene have been shown to lead to specific cellular alterations, specific mutations can lead to diverse phenotypic results as well, suggestive that other genetic or epigenetic factors may be involved (Lee et al. 2001). In a study by Meier et al. 2016, it was found that protein synthesis was equally impaired in mice models for both normal wild-type (WT) tau and mutant tau variants (P301L and ΔK280), suggestive that non-mutated tau can have similar repercussions as mutated tau, diminishment in protein synthesis.

Tau phosphorylation has been found to occur on roughly 25 serine and threonine residues located outside the region where tau binds to microtubules (Cohen et al. 2011), with half of these being phosphorylated via protein kinases such as members of the MAP kinase, cyclin-dependent kinase, and glycogen synthase kinase 3 families (Jin et al. 2011). It is noted in Jin et al. 2011 that when tau comes into contact with natural oligomers such as Aβ dimers, it is possible to induce hyperphosphorylation, with this phenomenon occurring even when synthetic, non-AD related dimers were employed, though to a less significant extent.

Neurofibrillary tangles (NFTs) form in a process of tau aggregation after tau has become hyperphosphorylated (Hoffmann et al. 2013). This both decreases its normal functional ability of binding to microtubules, as well as causes its subsequent transport to the somatodendritic region, where it assembles into filaments (Rizzu et al. 1999; Hoffmann et al. 2013). NFTs have long been shown to positively correlate to the degree

of neurodegeneration found in AD patients (Lee et al. 2001). In models where mice overexpressed WT human tau, however, NFTs were not found in cells before widespread neuron death occurred (Rocher et al. 2010). Additionally, NFTs do not necessarily lead to alterations in spine morphology, electrophysiological properties, or other characteristics noticed in neurons undergoing neurodegeneration (Rocher et al. 2010). In another study, it was noted that after transgenic tau was suppressed, memory function improved and neuron count stabilized, but NFTs continued to accumulate, suggestive that NFTs on their own do not cause cognitive or neuronal morphological symptoms for tauopathies (SantaCruz et al. 2005).

Pathogenic Impact of Mutant Tau on Synapses

Because synapses are located a relatively great distance from the neuron soma, and because they therefore rely on microtubule transport of materials, any disruption in this process can lead to negative effects regarding normal synaptic function (Yoshiyama et al. 2007). Excess mutant tau has been shown in studies to cause reduced binding to microtubules, increasing inefficiency in transport of materials from soma to synapse via axons (Zhang et al. 2004). In P301S mice where mutant tau levels are roughly five times endogenous tau levels, the mutated tau is not capable of efficiently binding to microtubules, leading to weakening of the microtubule polymer and reduction of tau in the at synapses (Roy et al. 2005).

It is important to note that tau oligomers have been found to be neurotoxic whereas this finding does not necessarily apply to tau fibers or monomers (Lasagna-Reeves et al. 2011). Specifically, tau oligomers negatively impact the function of

synapses by reducing levels of synaptic vesicle-associated proteins synaptophysin and septin-11 as well as negatively impact mitochondrial function by decreasing levels of NADH-ubiquinone oxidoreductase (Lasagna-Reeves et al. 2011). Tau oligomers have also been shown to activate caspase-9 resulting in apoptosis via the mitochondrial pathway (Lasagna-Reeves et al. 2011). Interestingly, oligomers of other proteins such as synuclein or insulin were not found to downregulate ribosomes, suggestive that tau has a specific means of interacting with ribosomes resulting in protein downregulation of products crucial for synaptic function (Meier et al. 2016).

Pathogenic Impact of Mutant Tau on Axonal Transport

Although tau is crucial in promoting microtubule stability, it can also have a negative impact on axonal transport through microtubule utilization. Stamer et al. 2002 reported that tau inhibits transport of organelles such as peroxisomes and mitochondria as well as Golgi-derived vesicles. In part, this could make neurons more susceptible to oxidative stress, especially at distal portions from the cell soma if peroxisomes are not able to be transported to this region (Stamer et al. 2002). Stamer et al. 2002 notes that tau aggregation is not dependent for this phenomenon to occur; simply overexpression of normal tau is sufficient to negatively impact microtubule stabilization, leading to decrease in transport of necessary organelles and vesicles. Jin et al. 2011 noted similar findings, showing cytoskeletal abnormalities were inhibited if endogenous tau was knocked down, but found acceleration of cytoskeletal abnormalities when WT human tau was expressed. Decreasing tau was also shown to benefit axonal transport in AD models by preventing the negative inhibitory effect of Aβ oligomers on axonal transport (Vossel

et al. 2010). Finally, acetylation has been shown to prevent tau from binding to microtubules, thus negatively impacting microtubule stability. Evidence for this is that tau acetylation has been detected on four lysine residues, three of which comprise the microtubule-binding repeat region (Cohen et al. 2011). It has been suggested that tau phosphorylation could then allow for suitable protein structure in the MT-binding region to become acetylated, thus inhibiting tau's capability of binding and stabilizing microtubules (Cohen et al. 2011). Other evidence regarding the critical role that acetylation plays in tau-microtubule association is related to the understanding that lysine deacetylase enzymes such as SIRT1 are significantly reduced in AD neurons and knocking down SIRT1 results in elevated levels of tau that are acetylated, suggestive that tau acetylation can play a negative role in tauopathies (Min et al. 2010).

Pathogenic Impact of Tau on Protein Synthesis

Because memory formation is dependent on protein synthesis, it follows that transcription or translation as well as errors in ribosomal function could play a role in symptom development in tauopathies. Ding et al. 2005 has noted that in AD patients, ribosomal function appears to be impaired in cortical regions, observing decreased rates of protein synthesis alongside decreased rRNA and tRNA levels as well as increased RNA oxidation. Interestingly, these findings occurred in individuals suffering only from MCI (which often precedes AD), suggestive that this decrease in protein synthesis is independent of later diagnostic findings common in AD such as NFTs or neuritic plaques (Ding et al. 2005). Although tau has been shown to interact with ribosomes, impairing protein synthesis by preventing translation factors from interacting with the ribosome, tau

has not been found to negatively interfere with elongation or initiation factors (Meier et al. 2016). Tau has also been shown to indirectly downregulate translation by causing chronic activation of the protein kinase RNA-like endoplasmic reticulum kinase (PERK) resulting in phosphorylation of the α subunit of eukaryotic translation initiation factor 2 (Eif2α) (Meier et al. 2016; Marciniak et al. 2006). Because proteins necessary for proper synaptic function are also reduced (such as PSD-95), the pathogenicity of tau protein interaction with ribosomes can also negatively impact synaptic function (Meier et al. 2016).

Pathogenic Impact of Tau on Spines

The majority of studies examining tauopathy mouse models have shown spine density to decrease (Hoffmann et al. 2013). However, as observed by Dickstein et al. 2010, many studies showing alterations in spine density employed transgenic mutated tau, whereas when non-mutated tau is expressed, there appears to be no difference in spine density when comparing human tau (htau) to endogenous tau in WT mice. A review article by Luebke et al. 2010 noted a study of pyramidal cells, conducted with the rTg4510 mouse model—a transgenic mouse model causing overexpression of mutant tau—found a 30 percent reduction in spine density. For this study, an alteration in spine shape was noted: there was an overall decrease in mushroom and stubby spines, while simultaneously witnessing an increase in thin spines (Luebke et al. 2010). Additionally, it was noted that dendritic volume had a strong relationship with spine number, hinting that in order to preserve spine count, the neuron will adapt by lengthening its dendritic processes to increase spine volume. Functionally, having a higher percentage of large

spines in comparison to small spines allows for retention of long term memories while inhibiting formation of new memories (Xu et al. 2014). This reinforces findings which have shown that mice with tauopathies have difficulty learning new maze routines in comparison to WT mice (Xu et al. 2014).

Loss of spine density may also be due to surrounding neuron loss. For example, Hoffmann et al. 2013 notes that tauopathies can cause loss of GABAergic interneurons in homozygous P301S Tau mice. Because these neural inputs would be inhibitory, to maintain homeostasis, a compensatory decrease in excitatory synapses may be required, consequently causing a decrease in overall spine density (Hoffmann et al. 2013).

Spine shape has also been shown to be altered during tauopathies. After spine density decreases, remaining apical tuft dendrites of cortical layer V were found to be longer and have a larger head volume, resulting in an increase in mushroom spine percentage compared to thin spines (Hoffmann et al. 2013). Hoffman et al. 2013 argues that rationale for this increase in spine size during overall spine density loss would allow for surface area to remain closer to homeostatic levels, thus allowing for an attempt to increase synaptic connections.

Hyperphosphorylated tau first accumulates in dendritic spines (Hoover et al. 2010). Specifically, tau appears to be vulnerable for hyperphosphorylation on specific serine or threonine residues, and interestingly, if phosphorylation can be prevented, tau loses its capacity to relocate into dendritic spines (Hoover et al. 2010). If soluble hyperphosphorylated tau makes it to dendritic spines, however, the hyperphosphorylated tau impairs glutamate receptor trafficking and synaptic anchoring, thus leading to an

overall disruption of synaptic function by suppressing AMPAR-mediated synaptic responses as well as NMDA receptors (Hoover et al. 2010). It is important to note that although hyperphosphorylated tau has been shown to accumulate in dendritic spines in some cell populations such as CA3 hippocampal neurons, this is not always the case as there have been findings of htau being absent from spines despite accumulating elsewhere in the somatodendritic portion of neurons (Hoffmann et al. 2013). Reasoning for this may be due to the spine's architecture: if the spine is supported by microtubules instead of actin filaments, this may facilitate htau accumulation due to its association with this cytoskeletal element as compared to actin (Hoffmann et al. 2013). It is interesting to note that protein kinases may play a role in the development of abnormal spine morphology and synapse deficiencies. A study by Tagawa et al. 2015 showed that inhibiting myristoylated alanine-rich C-kinases substrate (MARCKS) or by inhibiting the two protein kinases that are directly involved in phosphorylation of MARCKS, protein kinase C (PKC) and calmodulin-dependent kinase (CamKII), allowed for return of normal spine formation.

Review of Stress Granules

Stress granules (SGs) form when a cell comes under stress, such as what occurs in neurodegenerative tauopathies (Wolozin, 2014). SGs contain a large number of components: preinitiation factors, mRNA, mRNA-binding proteins (RBPs) such as TIA and TTP, proteins for mRNA metabolism such as G3BP, and signaling proteins (Kedersha and Anderson, 2007). In a nonpathogenic setting, SGs form through a complex process linked to some form of cellular stress, during which elongation initiation factor

2α (eIF2α) becomes phosphorylated and ribosomes along with initiation factors dissociate (Wolozin, 2012). Following this, RBPs bind to free, circulating mRNA, initiating the SG formation process; this process continues as more mRNA and RBPs accumulate, increasing the mass of the developing SG (Wolozin, 2012). eIF2α phosphorylation acts as a key regulatory component for allowing RBPs to amass with other cellular components (Wolozin, 2012) as well as inhibiting translation initiation (Buchan and Parker, 2009). The overall effect from SG formation is that cellular resources are conserved for essential proteins by suppressing, silencing, or degrading non-essential protein translation (Wolozin, 2014) as well as allocating non-essential mRNA transcripts for utilization in SGs (Vanderweyde et al. 2013). SGs also play a role in determining whether stress is extreme enough for a cell to undergo apoptosis. SGs possess apoptotic regulatory proteins, effectively inhibiting these proteins from interacting with additional factors to promote apoptosis, thus inhibiting apoptosis in response to stress (Buchan and Parker, 2009).

Overall, SG function appears to be protective; during stress, they seize mRNA that would not be useful for the cell, allowing protein translation that serves an overall protective role for the cell, such as inhibiting apoptosis, to be promoted (Vanderweyde et al. 2013). Additionally, via utilization of TTP—an RBP—SGs assist in degradation of mRNAs via nearby processing bodies (Vanderweyde et al. 2013). SGs are important in the synapse where they regulate production of synaptic proteins such as PSD-95 and GluR (Liu-Yesucevitz et al. 2011). Evidence suggests that SGs use cytoskeletal

microtubules to reach distance places in the cell such as the axonal synapse of a neuron (Knowles et al. 1996).

Although SGs for the most part are beneficial to cells by helping cope with stress, pathogenic effects can precipitate when SGs endure for a lengthy, sustained time. For example, by creating an environment of compact, highly dense proteins, a suitable environment for forming oligomers and fibers may occur (Wolozin, 2012). Additionally, if SGs persist despite a lack of a stressful environment, negative impacts from sustained loss of normal protein translation due to loss of RBPs or free mRNA could also negatively impact the cell (Wolozin, 2012). In diseases where tau inclusions exist, such as frontotemporal dementia with parkinsonism-17 (FTDP-17) and Alzheimer's disease (AD), it has been shown tau co-localizes with SGs, potentially causing increased tau accumulation in the cell (Vanderweyde et al. 2013). Evidence also suggests that in addition to SGs stimulating development of phosphorylated tau inclusions (Vanderweyde et al. 2012), tau appears to reciprocally stimulate SG formation (Vanderweyde et al. 2013). Interestingly, in many cases of neurodegenerative tauopathies, SG inclusions actually display greater density than NFTs, suggesting that total pathological inclusions in a neuron are much greater than regions simply containing tau protein (Vanderweyde et al. 2013). It should be noted that the specific RBPs present in an SG determine the pathological properties of the SG (Vanderweyde et al. 2012).

Review of RNA-Binding Proteins

Overall, RBPs have two conserved motifs providing their function: a component that allows them to bind to RNA and a component that contains a large proportion of

glycine amino acids, allowing for interaction with other proteins due to strong hydrophobic interactions (Wolozin, 2014; Vanderweyde et al. 2013). Their RNA-binding component allows RBPs to regulate the translation of mRNAs by providing stability to the transcript, specifically by binding to an untranslated or coding region (Liu-Yesucevitz et al. 2011). In the non-stress state, RBPs exist both in the nucleus, where their function is for mRNA maturation including helicase function, splicing, nuclear export, and RNA polymerase elongation; however, in a stressed-state, RBPs leave the nucleus for the cytoplasm where their main function is to mainly inhibit the translation process by binding to free mRNA, in turn causing the formation of SGs (Vanderweyde et al. 2013).

It is important to realize that RBPs function as critical pathways in local RNA translation and mutations in these proteins often results in a specific neurologic disease (Liu-Yesucevitz et al. 2011). Diseases linked to mutations in RBPs include amyotrophic lateral sclerosis (ALS), frontotemporal dementia, and spinal muscular atrophy, and play a role in other diseases such as AD and Creutzfeld-Jacob disease (Vanderweyde et al. 2013). Mutations resulting in disease generally either influence granule aggregation or mRNA processing (Liu-Yesucevitz et al. 2011). For example, TDP-43 normally assists delivery of mRNA transcripts via microtubule transport to different regions of the neuron; specific mutations for TDP-43, however, have been linked to specific neurodegenerative diseases, such as ALS (Alami et al. 2014).

One example on an RBP implicated in neurodegenerative tauopathies is TIA-1. This RBP normally functions by targeting C-rich and U-rich mRNA transcripts and represses translation of these transcripts (Vanderweyde et al. 2013). Examples of

transcripts impacted include TNF-α and COX-2 (Vanderweyde et al. 2013). Based on the inflammatory function of these proteins, suppression of TIA-1 results in auto-inflammatory symptoms, such as mild arthritis (Phillips et al. 2004). When mutated to not have its RNA-binding domains, TIA-1 inhibits SG formation (Kedersha et al. 1999). In tauopathies, TIA-1 has been shown to bind to tau protein and that if TIA-1 is overexpressed, this may cause increased formation of hyperphosporylated tau inclusions (Vanderweyde et al. 2012).

Therapeutic Options for Tauopathies

Currently, most treatment options for neurodegenerative ailments such as AD are only capable of managing symptoms, and generally only for a short timeframe (Meier et al. 2016). Because atrophy in the brain is a major symptom, neuronal loss is inevitable in most diseases (deToldeo-Morrell et al. 2007). For this reason, one of the main therapeutic options is providing neurotransmitters to patients since individuals lose the ability to generate neurotransmitters with neuronal loss (Selkoe, 2001). One of the most useful supplements for treatment of conditions like AD being acetylcholine (Selkoe, 2001).

As was shown earlier with AD, neuronal atrophy can be quite significant before clinical symptoms become apparent (deToldeo-Morrell et al. 2007). For this reason, one method crucial for treating most tauopathies would be early detection through biomarkers. Glodzik et al. 2011 noted that biomarkers in cerebral spinal fluid (CSF) may be able to perform this task, noting that elevated hyperphosphorylated tau was found to be linked to both a decrease in declarative memory and neuronal loss of the medial temporal lobe; it should be noted that hyperphosphorylated tau has been shown to have a

positive correlation with age, especially in older populations (Jaworski, et al. 2009). Additionally, it has been noted that some neurodegenerative diseases such as AD usually begin with MCI. Being able to predict if MCI will progress to AD would be beneficial as treatment options could begin earlier, potentially delaying progression of MCI to AD (Ewers et al. 2012). Testing for potential biomarkers that would predict this disease progression, Ewers et al. 2012 noted that the best model was a high tau/*A*β ratio paired with clinical testing showing decreased performance in immediate and delayed recall. Finally, in tauopathies, tau can become mutated, preventing them from binding to and stabilizing microtubules. If drugs can be generated that can help stabilize microtubule polymerization to allow for little disruption in axonal transport, this could help alleviate many of the morphological changes seen in neurons due to dendrites not being able to receive necessary resources (Roy et al. 2005). Finally, drugs that deacetylate tau lysine residues could be therapeutic as it has been shown that tau acetylation has a role in pathological tau transformation (Cook et al. 2014).

Purpose of Study

The purpose of the present study is to analyze the morphological impact that tau can have on dendritic processes for neurons. The entorhinal cortex will be the region studied since important diseases such as AD are known to cause symptoms of neuron atrophy in the early course of the disease. Additionally, fan and stellate cells will be compared to identify if they respond differently in tauopathies. The present study employed the P301S mouse model, a genotype containing a tau gene mutation resulting in FTDP-17 at an advanced rate. Previous studies have shown this genotype to have a

decrease in synapse density in the hippocampus at three months, tau plaque formation at six months, and finally neuronal atrophy in the hippocampus and entorhinal cortex by twelve months (Yoshiyama et al. 2007). The P301S model overexpresses mutant tau by roughly five times compared to endogenous tau expression (DeVos et al. 2017), useful for analyzing the effect that overexpression of tau can have on neuron function and morphology. In contrast to WT tau, this mutation was found to decrease binding capacity and binding affinity for microtubules, a crucial pathogenic property of tauopathies (Hong et al. 1998).

METHODS

Mice Used in the Study

The P301S mouse model of tauopathy with TIA1 knockdown was used in this study. Brain slices were prepared from the following two genotypes of mice: P301S tau (-/-), TIA1 (+/+) (namely wildtype or WT) and P301S tau (+/-), TIA1 (+/+); the specific ages and genders for each of the six mice studied is in Table 1. Mice were provided and cared for in the Laboratory Animal Science Center of the Boston University Medical Center. All animals were managed under guidelines from the American Association for the Accreditation of Laboratory Animal Care. Additionally, all procedures were done under strict animal care guidelines from the NIH *Guide for the Care and Use of Laboratory Animals and the U.S. Public Health Service Policy on Humane Care and Use of Laboratory Animals.*

Table 1: Genotype, gender, and age of each mouse utilized in study

Genotype	Gender	Age
P301S tau (-/-), TIA1(+/+)	Female	6.3 months
P301S tau (-/-), TIA1(+/+)	Male	6.5 months
P301S tau (-/-), TIA1(+/+)	Male	6.5 months
P301S tau (-/-), TIA1(+/+)	Male	6.6 months
P301S tau (+/-), TIA1 (+/+)	Female	6.5 months
P301S tau (+/-), TIA1 (+/+)	Male	6.5 months

Perfusion/Preparation of Brain Slices

Mice were first anesthetized with isofluorine and then euthanized via decapitation, allowing for removal of the brain. The brain was placed in ice-cold Ringer's

Solution (124 mM NaCl, 1.0 mM KCl, 2.0 mM KH_2PO_4, 1.3mM $MgCl_2$, 2.5 mM $CaCl_2$, 10 mM Glucose) and then sectioned into 300 μm slices using a vibratome after mounting on an agar slab. The specific slices incorporated for this study included neurons from the medial entorhinal and lateral entorhinal cortices, with the majority of neurons coming from the lateral entorhinal cortex. The slices were then placed in room temperature oxygenated Ringer's solution and left for one hour to equilibrate.

Electrophysiological recordings (a discussion of which is beyond the scope of this thesis) were conducted on the neurons visually identified using a Nikon E600 infrared-differential interference contrast (IR-DIC) microscope (Micro Video Instruments, Avon, MA). This process utilized a submersion recording chamber (Harvard Apparatus, Holliston, MA) where tissue slices were stabilized and continuously supplied with a flow of oxygenated Ringer's solution. Neurons were injected with 0.5% biocytin during the recordings.

The neurons filled with biocytin during electrophysiological recordings were fixed in 4% paraformaldehyde and incubated overnight. Following this, tissue slices were rinsed in 0.1 M phosphate buffered saline (PBS) buffer solution three times for ten minutes each and then washed in a buffer containing 1% Triton X-100 for 2 hours at room temperature to increase permeability of tissue slices. Slices were then labeled using streptavidin fluorescent conjugates—specifically Alexa-Streptavidin Fluor 488 (1:500, Life Technologies)—for two days at 4°C. Following this, slices were again rinsed three times in 0.1M PBS buffer solution, and then stored in PBS-Azide, and eventually transferred into an anti-freeze solution to complete the process.

Confocal Imaging

Neurons were scanned in 3D with a high-resolution Zeiss 510 Confocal Laser Scanning Microscope (CLSM), with a 20x 0.5 NA water-immersion objective lens. During imaging, a 488 nm laser powered at approximately 30% (29.5-30.4%) was used to excite the fluorophores located within the neuron, with the detection range of the excitation/emission curve wavelength ranging from 493 nm-560 nm. For the image collected, a resolution of 2048 x 2048 pixels was used; this, along with setting the z-stack size at 0.5 µm, resulted in an overall resolution of a 0.26869 x 0.26869 x 0.5 µm voxel size to produce the image for analysis of the morphological characteristics of dendrite and soma. During all image processing, the microscope incorporated a scanning speed of 400Hz and a detection pinhole set at 1 Airy Unit.

While imaging individual neurons, the X-, Y-, and Z- planes were set to ensure the entirety of the neuron's dendrites would be incorporated into the image. After determining these parameters, the amount of saturation was adjusted roughly every 10 µm in the Z-plane to ensure that dendrites would be adequately imaged; this process consisted of attempting to saturate the image to the extent that one pixel of a dendrite would have a degree of oversaturation at each Z-stack. Additionally, the offset of the image was adjusted every 10 µm to ensure that background was minimized; this process consisted of ensuring that all true black spaces were recognized while also ensuring that no artificial black spaces disrupted dendritic integrity.

The acquired confocal images were then deconvolved with AutoQuant software (Media Cybernetics, Bethesda, MD) to reverse optical distortion in the z plane, allowing

for clearer images of the neuronal dendrites; an example of the restoration effect is shown in Figure 4. This was necessary to adjust for the scattering of light that could contribute to increased background noise. Following this, the files were converted from 16-bit to 8-bit .tif files allowing for dendrite and soma reconstruction using NeuroLucida 360 (MBF, Vermont).

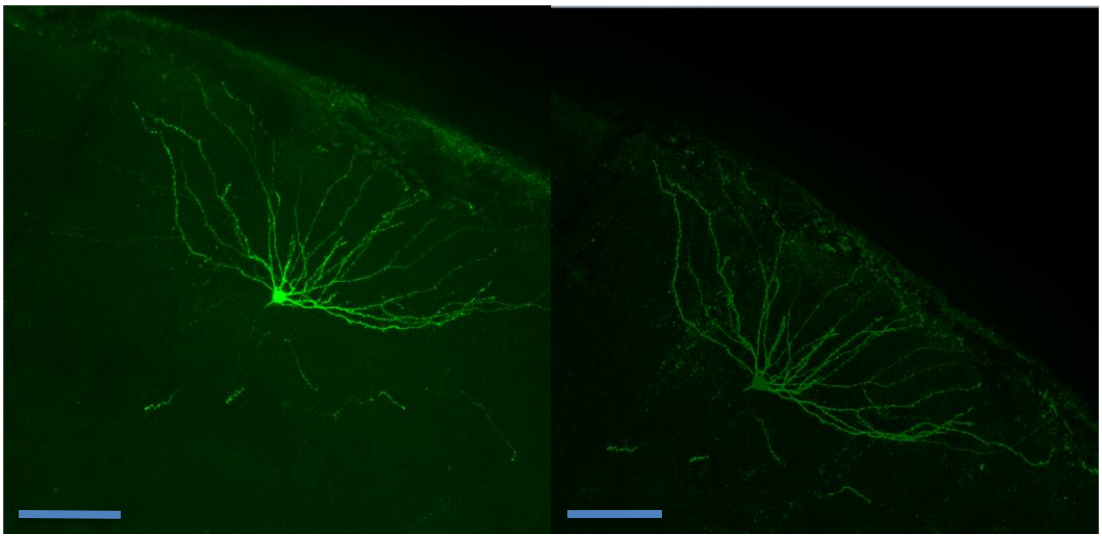

Figure 4. Example of a confocal image before (left) and after (right) deconvolution utilizing AutoQuant software. The neuron used in this example is Feb2IR1d. Scale bar: 100 µm.

Neuron Reconstruction

Image stacks were loaded into NeuroLucida 360 for reconstruction of the neuron cell bodies and dendrites. Dendrites were reconstructed using a semi-automated user-guided tracing mechanism, while the soma was reconstructed via an automatic mechanism, determining the soma's volume. Upon completion, the files were loaded into the 64-bit version of NeuroLucida where manual inspection took place to ensure that all dendrites were reconstructed accurately as well as to ensure that no dendrites were

missed in the reconstruction process. Additionally, information that would be incorporated into analysis was confirmed, such as ensuring correct nodal points where dendrites branch were accurate. An example of a neuron after complete reconstruction and editing can be seen in Figure 5.

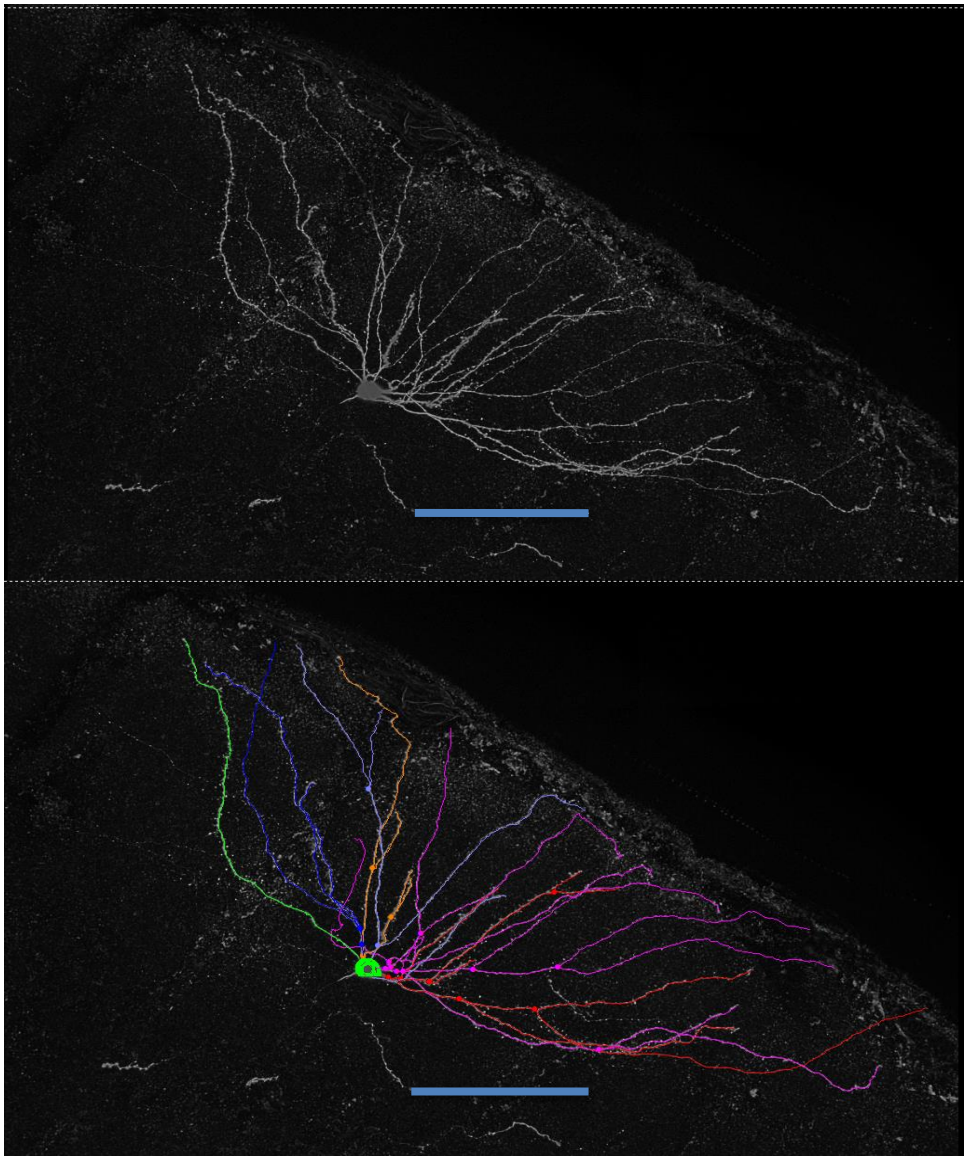

Figure 5. Representation of a neuron before and after reconstruction and editing using NeuroLucida. The image on the left is of an unaltered 8-bit image file in NeuroLucida 360 program before any neuron reconstruction has commenced. The image on the right shows what the neuron looks like after it has been reconstructed and edited. The neuron used in this example is Feb2IR1d. Scale bar: 100 µm.

Neuron Analysis

Neurons were analyzed using NeuroLucida Explorer. Morphological features of analyzing the branched structure of the neuron including, for example, description of nodal positions, straight line distance of individual dendrites, and dendrite tortuosity. Additionally, Sholl analysis was conducted to provide an overview of dendrite branch length, dendritic surface area, and number of dendritic intersections in relation to a set of concentric spheres centered at the cell body. Finally, a convex hull analysis, an operation used to map out the volume or surface area of an object by creating a polygon that encompassing all points inside of constructed shape, was employed, useful for acting as a model for understanding the amount of overall physical space taken up by the neuronal dendrites.

Statistical Analyses

Microsoft Excel was used for organizing data both for statistical analysis and graphical representation. Homoscedastic, non-paired t-tests were used when assessing for statistical significance which was defined for a p-value being less than 0.05.

RESULTS

Morphological data was obtained from 29 neurons in the lateral entorhinal cortex of the mouse. Visual inspection was used to determine if a neuron could be classified as a fan cell, stellate cell, or some other type of neuron based on characteristic features of the neurons reported in the literature (Alonso and Kirk, 1993; Canto et al. 2008; Marcantoni et al., 2014; Tahvildari and Alonso, 2005). Of the total number of cells recorded, 13 came from the P301S tau (+/-), TIA1 (+/+) genotype (which was designated "tau") and 16 came from the P301S tau (-/-), TIA1 (+/+) genotype (which was designated "WT"). Of the cells recorded in the tau mice, five were fan cells, five were stellate cells, and three were cells of some other classification (multipolar, horizontal tripolar, and pyramidal). Of the cells recorded in the WT mice, five were fan cells, ten were stellate cells, and one cell was of some other classification (oblique pyramidal). Based on the number of cells available, morphological analysis and comparisons were made for neurons based on their genotype (tau or WT) as well if their neuron classification was that was considered to be either a fan cell or stellate cell.

Visual Morphological Analysis of Neurons

The reconstructed fan cells had a typical appearance in that their dendrites did not diverge from the soma in a uniform, multidirectional pattern; instead, dendrites tended to branch in a horizontal manner as well as orthogonal in one direction to this plane. An example of an ideal representation of a fan cell is shown for Feb2IR1d in Figure 6 where these dendrites are heading towards the pia. This was not always the case as sometimes a few dendrites would branch opposite in the direction of the pia (e.g. Feb4IR1b,

Mar9IR2h; Figure 6), but upon closer inspection, it was noted that dendrites heading towards the pia outnumbered dendrites heading in the opposite direction, which is also noted in the literature that fan cells may possess a few dendrites which branch in this pattern (Tahvildari and Alonso, 2005). Stellate cells, on the other hand, branch in a more uniform and equidistant pattern from the soma. These neuron's dendritic branching characteristics can be appreciated in Figure 6.

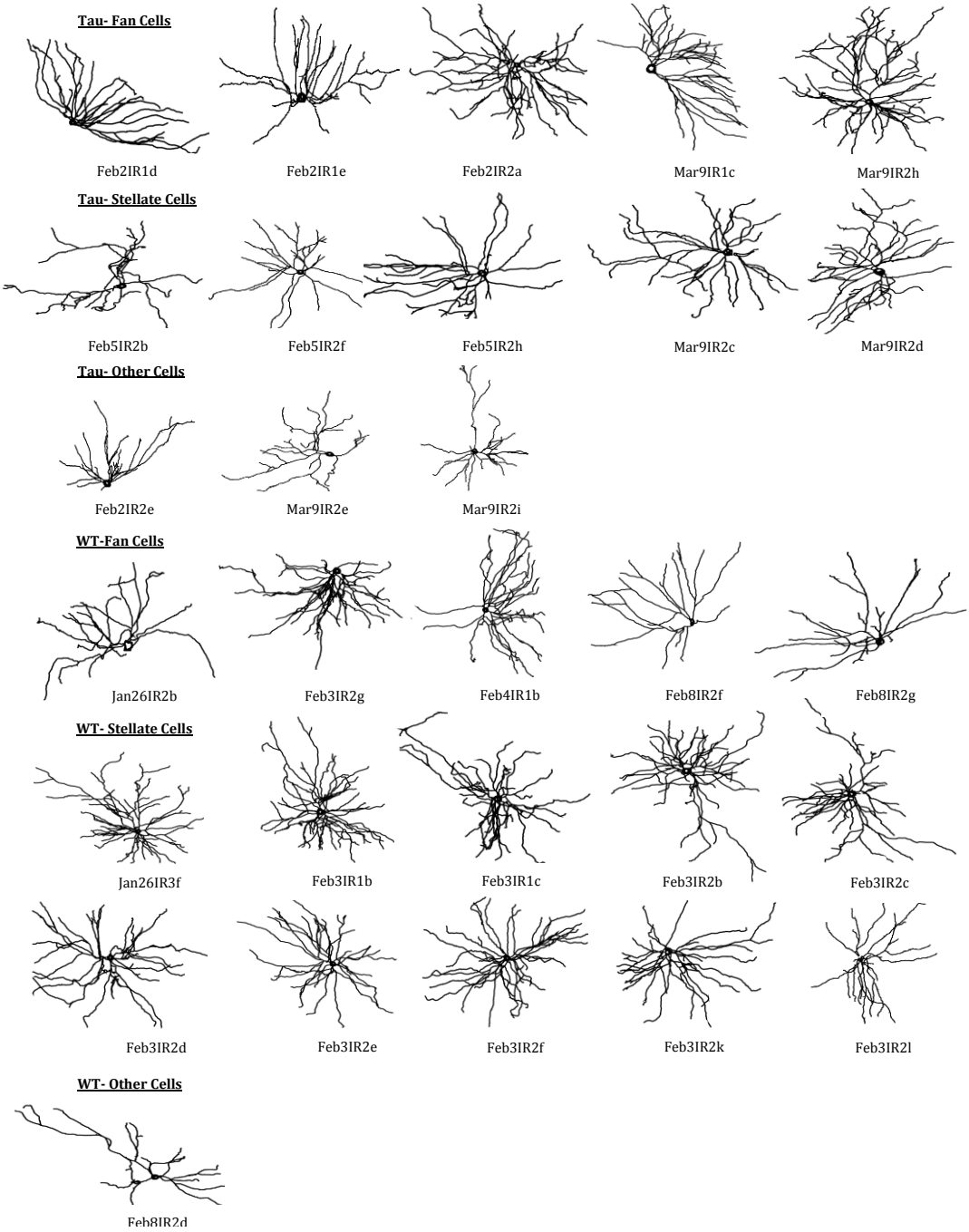

Figure 6. Three-dimensional projection of tau (P301S tau (+/-), TIA1 (+/+)) and WT (P301S tau (-/-), TIA1 (+/+)) neurons used in this study. Neurons are grouped by neuron classification. Their Cell ID's are provided under the image. Images were assembled using Illustrator from data collected via NeuroLucida Explorer.

Primary Dendrite Quantity Analysis

One measure of neural complexity is the number of individual primary dendrites branching off of the cell body. During neuronal reconstruction, primary dendrite counts were made. When sub-classifying the tau and WT neurons into categorical definitions of fan versus stellate cells based on morphological analysis of the confocal images taken, it was found that WT stellate cells on average had significantly more primary dendrites than tau stellate cells (8.4 ± 1.8 (n=10) vs 6.4 ± 1.1 (n=5), p=0.046) (Fig 7B). Interestingly, this trend differed in fan cells where tau fan cells were found to have a higher number of primary dendrites compared to WT fan cells (7.0 ± 1.4 (n=5) vs 5.2 ± 1.1 (n=5), p=0.055) (Fig 7B). As a whole, stellate cells on average were found to have a significantly higher count in primary dendrites compared to fan cells (7.7 ± 1.9 (n=15) vs 6.1 ± 1.5 (n=10), p=0.031) (Fig 7A). This trend continued to a greater extent when solely analyzing WT neurons where the average primary dendrite count difference jumped to 8.4 ± 1.8 (n=10) vs 5.2 ± 1.1 (n=5), p=0.004 (Fig 7B). On the other hand, this trend of stellate cells having a greater number of primary dendrites was lost entirely when analyzing solely tau cells as tau fan cells were actually not found to have a difference in number of primary dendrites compared to tau stellate cells (7.0 ± 1.4 (n=5) vs 6.4 ± 1.1 (n=5), p=0.481) (Fig 7B).

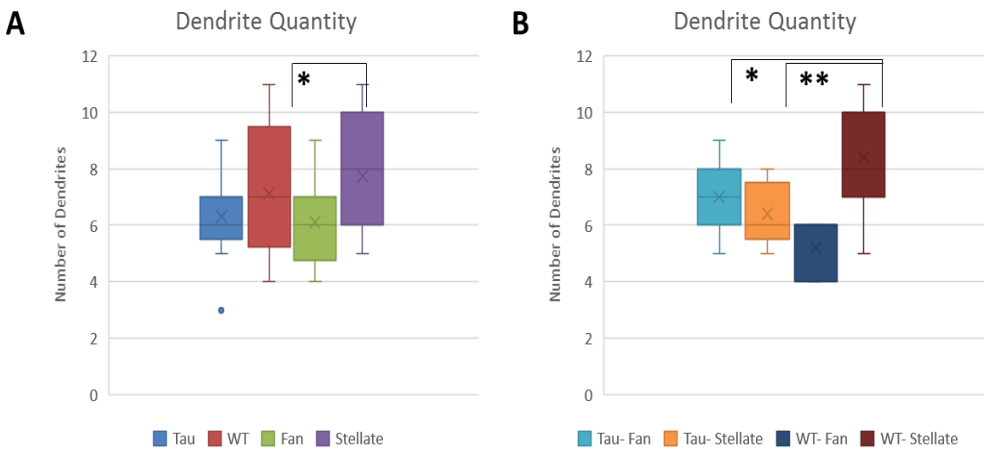

Figure 7. Box and whisker plots of the average primary dendrite number based on neuron classification and/or genotype. A) The average primary dendrite quantity for tau, WT, fan, or stellate neurons. B) The average primary dendrite quantity for when differentiating by neuron classification *and* genotype. *p<0.05; **p<0.005.

Dendritic Node/Ending Analysis

To analyze the extent of dendritic branching, the quantity of nodes (representing the points at which the dendrite branches) and endings (representing the total end points of all dendrites) were quantified. Theoretically, the number of nodes and endings should be related, in the sense that endings should equal the sum of primary dendrites and nodes per neuron (E = N + D). Overall, node and ending quantity followed the same pattern among different neuron classifications as was found when analyzing primary dendrite quantity. That said, there were fewer statistically significant relationships, with no strong differentiation when comparing overall tau to WT neurons and when comparing fan to stellate cells (Fig 8 A,C). Two significant findings were that WT stellate cells possessed a higher number of nodes and endings than tau stellate cells (nodes: 37.9 ± 8.5 (n=10) vs

26.4 ± 7.5 (n=5), p=0.024; endings: 45.9 ± 9.5 (n=10) vs 33.0 ± 7.4 (n=5), p=0.020) (Fig 8 B, D) and WT stellate cells having more nodes and endings than WT fan cells (nodes: 37.9 ± 8.5 (n=10) vs 24.2 ± 11.9 (n=5), p=0.023; nodes: 45.9 ± 9.5 (n=10) vs 29.4 ± 12.0 (n=5), p=0.012) (Fig 8 B,D). Tau fan cells were not found to have more nodes and endings than tau stellate cells, despite tau fan cells possessing more primary dendrites (Fig 8 B, D).

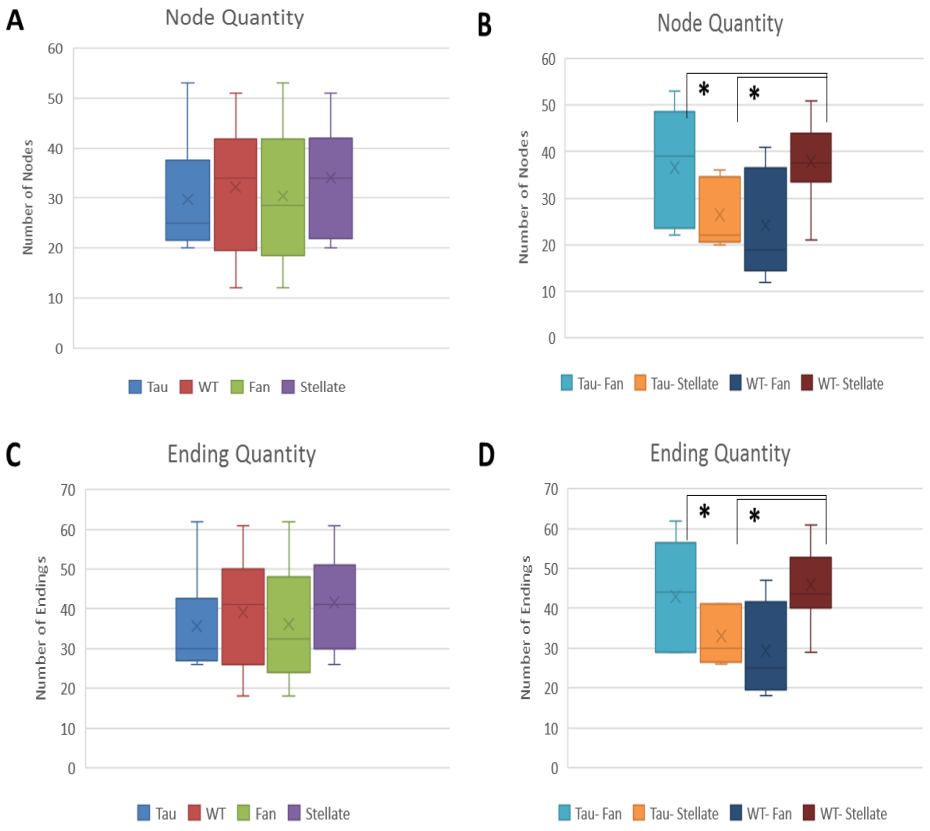

Figure 8. Box and whisker plots of the node and ending count based on neuron classification and/or genotype. A) The average node count for tau, WT, fan, or stellate neurons. B) The average node count for when differentiating by neuron classification *and* genotype. C) The average ending count for tau, WT, fan, or stellate neurons. D) The average ending count for when differentiating by neuron classification *and* genotype. *p<0.05.

Dendritic Length Analysis

Total dendritic length between Tau and WT or fan and stellate cell did not differ (Fig 9A). Additionally, mean dendritic length also did not show a difference between Tau and WT neurons (Fig 9C); that said, fan and stellate cells overall did show a trend in differing with fan cells on average having longer dendrites when compared to stellate cells (997.3 ± 396.5 μm (n=10) vs 769.5 ± 269.8 μm (n=15), p=0.100) (Fig 9A). Taken together with the earlier finding of stellate cells as a whole having significantly more primary dendrites than fan cells, this data reveals that, with regard to the morphological features of the two neuron classifications, stellate cells possess on average more dendritic branches but have a shorter overall length, whereas fan cells possess fewer branching dendrites from the soma, but each of these dendrites has a longer average length. Functionally, this morphological pattern makes sense; the asymmetrical design of the fan cell where all dendrites branch apically towards the pia with no basal extensions would imply a smaller number of primary dendrites, and since neurons rely on dendrites for enhanced surface area for signal reception from neighboring neurons, assuming identical need for signaling, it makes sense that both neuron classifications would have similar overall surface area.

When sub-typing the WT and tau cells into their fan and stellate cell subclasses, a similar trend to what was observed for number of primary dendrites and number of nodes and endings was found for total dendritic length: on average, tau fan cells showed a trend of having a greater average total dendritic length when compared to WT fan cells (7047.6 ± 1540.6 μm (n=5) vs 4753.4 ± 2203.1 μm (n=5), p=0.093), and WT stellate cells were

found to have a significantly greater average total dendritic length compared to tau stellate cells (6354.7 ± 1642.0 μm (n=10) vs 4541.0 ± 1242.8 μm (n=5), p=0.050) (Fig 9B). It is also of interest to note that once again, the WT mouse model failed to differ in comparison when comparing the overall dendritic length of stellate cells to fan cells (6354.7 ± 1642.0 μm (n=10) vs 4753.4 ± 2203.1 μm (n=5) , p=0.135); on the other hand, in the tau mouse model, fan cells had a significantly greater total dendritic length compared to stellate cells (7047.6 ± 1540.6 μm (n=5) vs 4541.0 ± 1242.8 μm (n=5), p=0.022) (Fig 9B).

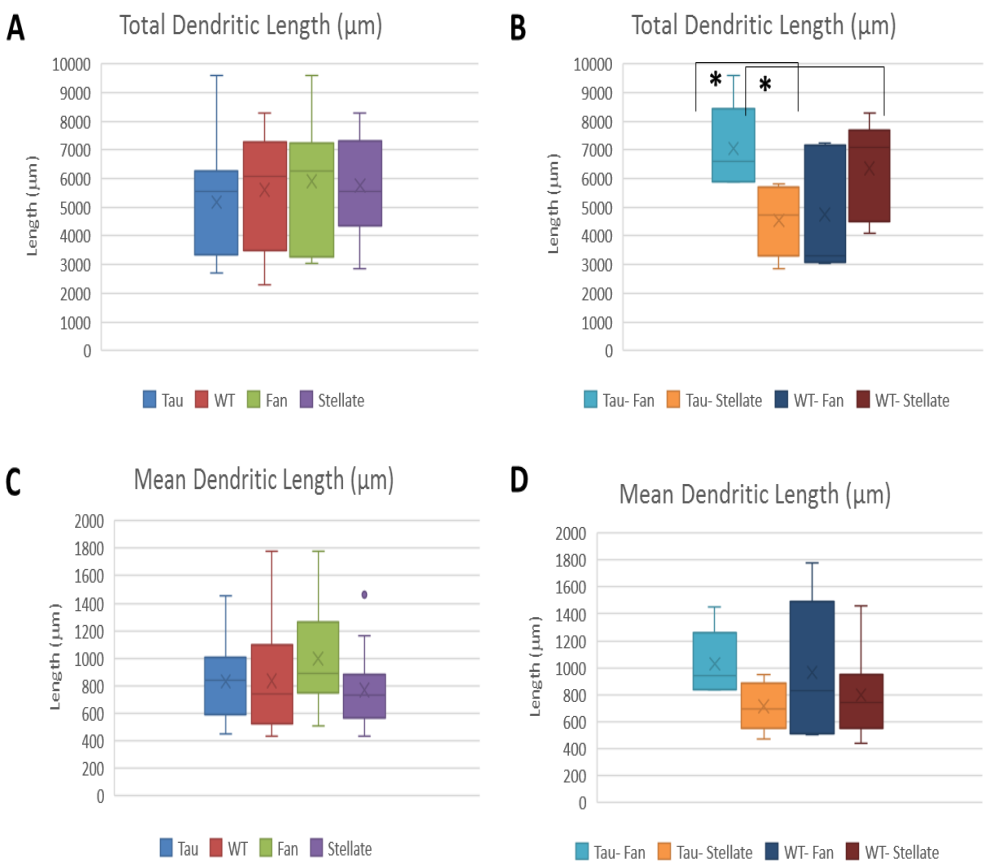

Figure 9. Box and whisker plots of the total dendritic length and mean dendritic length on neuron classification and/or genotype. A) The average total dendritic length for tau, WT, fan, or stellate neurons. B) The average total dendritic length for when differentiating by neuron classification *and* genotype. C) The average mean dendritic length for tau, WT, fan, or stellate neurons. D) The average mean dendritic length for when differentiating by neuron classification *and* genotype. *p<0.05.

Overview of Sholl Analyses

Sholl analysis is a quantitative method to characterize structural features of dendrites –their topology- by creating a system of concentric circles of increasing radius stemming from the cell body. By doing this, an overall assessment of dendritic arbor

complexity can be modeled. For this analysis, intersections, dendritic length, and surface area was conducted utilizing a radius of 10 μm for concentric rings.

Sholl Analysis: Intersections

Intersections are defined as dendrites crossing a radial concentric ring centered at the cell body of the neuron and extending in a somatofugal manner. This analysis can provide valuable information in terms of better understanding the complexity of dendritic branching: for example, if two neuron types were found to have roughly equal number of primary dendrites but one neuron type had a greater number of intersections close to the soma, that data could be suggestive that this neuron type may have a greater degree of dendritic branching closer to the soma.

When comparing WT and tau neurons, WT was found to have a significantly greater number of intersections between 20-50 μm from the soma, but after this point, intersections once again became roughly equal (Fig. 10A). By distinguishing between stellate cell and fan cell when comparing the WT and tau neurons, further trends were noted. Tau fan cells were shown to consistently have a higher number of intersections throughout the entire Sholl analysis when compared to WT fan cells, with large regions where this difference was statistically significant between 110-230 μm (Fig. 10C). Contrastingly, when analyzing only stellate cells, neurons from the WT genotype were shown to predominantly have more interactions throughout the Sholl analysis, with points of significant differences in the range of 20-50 μm from the somal center (Fig. 10 D).

When analyzing by neuron type, it was found that although stellate cells had a

significantly greater number of intersections between 20-50 μm from the soma compared to fan cells; this trend then reversed at a radius of 140-200 μm away from the soma with fan cells then having significantly higher number of intersections (Fig 10 B). This trend makes some sense since stellate cells were earlier shown to have a higher number of primary dendrites than fan cells (7.7 ± 1.9 (n=15) vs 6.1 ± 1.5 (n=10), p=0.031) which would aid that neuron type in possessing more primary dendrites to aid in branching to potentially inflate the amount of intersections near the soma. By 140 μm away from the cell body, however, the trend had reversed with fan cells now having a significantly higher number of intersections compared to stellate cells, suggestive that the degree of branching had increased for fan cells prior to this point between 60-130 μm in comparison to stellate cells. When analyzing solely WT neurons, stellate cells were found to once again possess this trait of having a significantly greater number of intersections close to the soma in comparison to fan cells (20-60 μm), though there was no significant difference in intersections between the two neuron types after this point (Fig. 10 F). Conversely, when analyzing tau cells, there was no early deviation in number of intersections between fan and stellate cells; that said, at roughly 110 μm away from the soma fan cells were shown to have a significantly greater number of intersections compared to stellate cells until roughly 220 μm away from the soma, with many differences between the two groups having a statistical significance where $p<0.005$ (Fig 10 E).

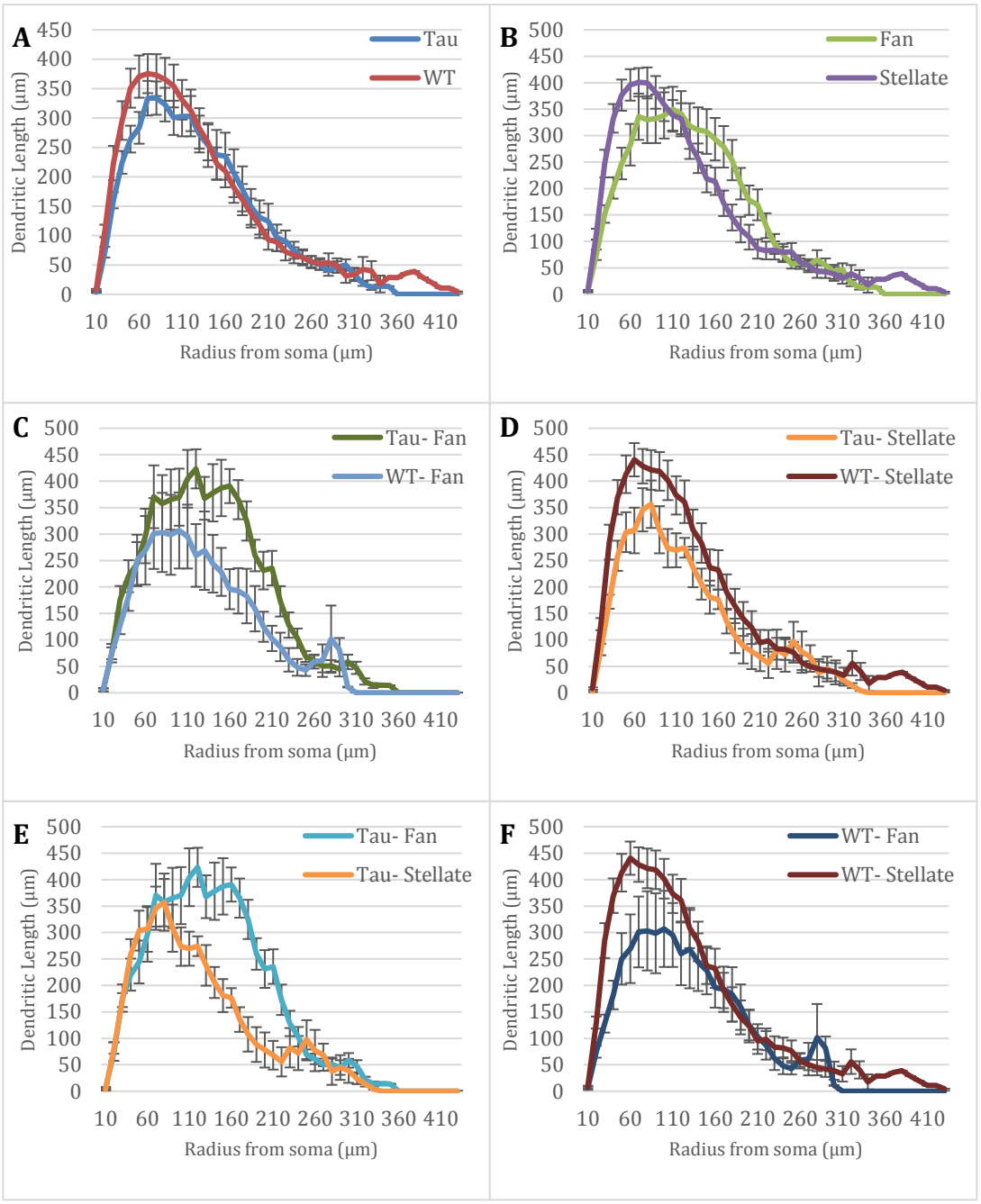

Figure 10. Intersection Sholl analyses comparison based on neuron classification and/or genotype. A) Sholl analysis of the total number of intersections in 10µm increments comparing tau and WT neurons. B-F were the same as in A except compared different neuron classifications and/or lineages. B) Comparison of fan and stellate cells. C) Comparison of fan cells by genotype (tau or WT). D) Comparison of stellate cells by genotype (tau or WT). E) Comparison of tau neurons by neuron classification (fan or stellate). F) Comparison of WT neurons by neuron classification (fan or stellate).

Sholl Analysis: Dendritic Length

Dendritic length in the Sholl context is defined as the length of dendrite located between each concentric ring. Overall, the results found when comparing neuron type and neuron genotype match closely to what was found when analyzing number of intersections; conceptually, this makes sense as a large factor for determining the number of intersections as well as overall length of dendrites would be the degree of branching. That said, any relative increase in dendritic length compared to intersection amount might suggest dendrites that curve at a tangential way to the concentric rings as opposed to dendrites that simply extend radially from the cell body.

When comparing cells by genotype, similar to what was found when analyzing for intersection amount, WT cells were found to have a greater overall dendritic length compared to tau cells close to the soma, but the difference was not as extreme when compared to analyzing number of intersections, with the difference only reaching statistical significance at one marker—20 μm from the soma (Fig. 11 A). When isolating by neuron type and then comparing neuron genotype, similar findings to what was found for intersection amount was again observed. Tau fan cells were once again observed to have a greater overall dendritic length compared to WT fan cells for the majority of the Sholl analysis, but these differences were not as extreme as when comparing the findings for intersection amount (Fig. 11 C).

When comparing neuron type, dendritic length was found to be greater in stellate cells compared to fan cells in regions closer to the soma (statistically significant between

20-60 μm), while the reverse trend of fan cells possessing greater dendritic length was found in regions further from the soma (statistically significant between 170-210 μm) (Fig. 11 B). Looking only at WT neurons, the trend of stellate cells possessing longer average dendritic length close to the soma continued (statistically significant between 20-50 μm), however after this point total dendritic length remained roughly similar for both stellate and fan cells (Fig. 11 F). When analyzing only tau neurons, there was no difference in dendritic length close to the soma. As the radius moved further from the soma, however, fan cells began to show a significantly larger dendritic length compared to stellate cells (statistically significant between 120-220 μm) (Fig. 11 E).

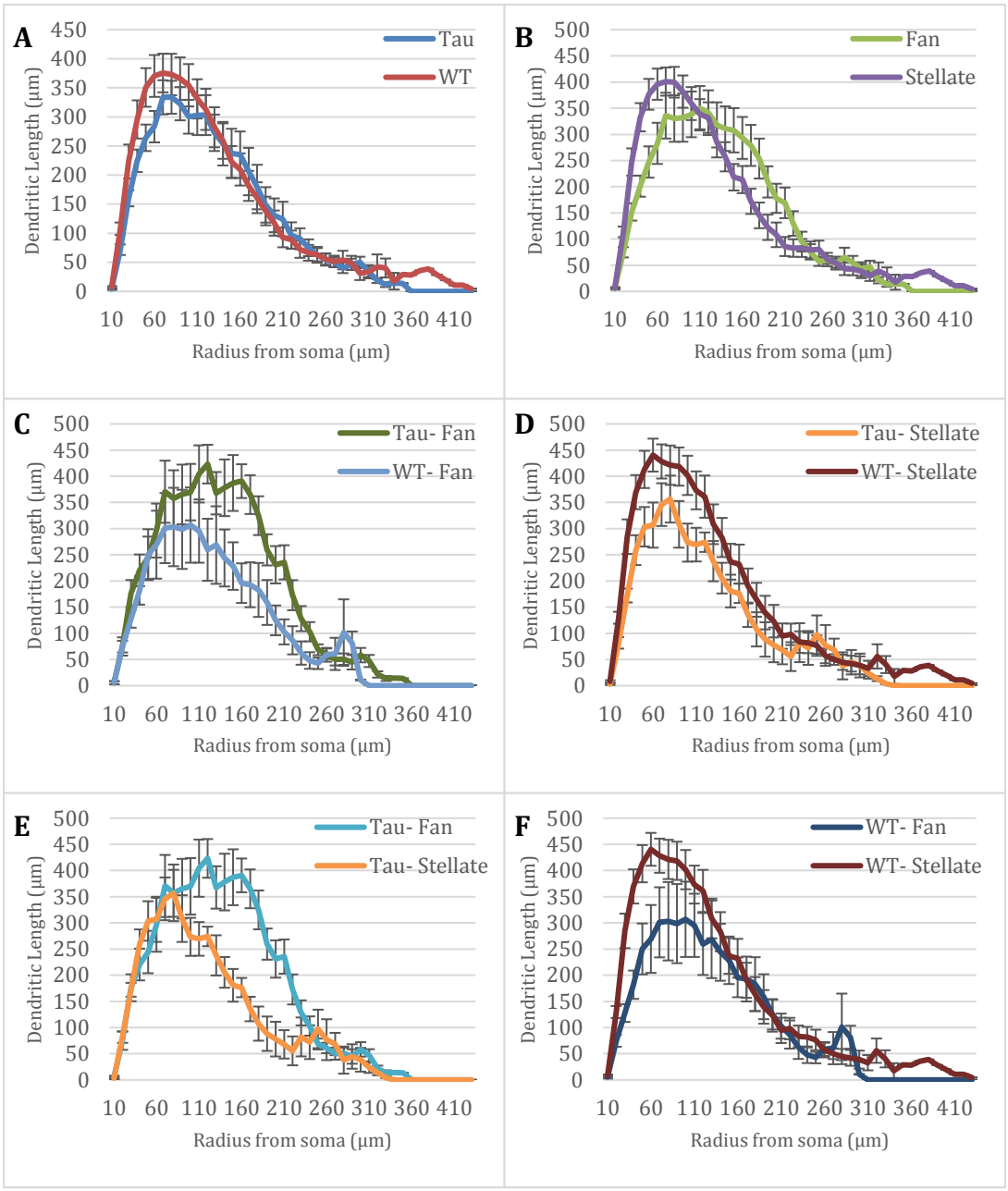

Figure 11. Dendritic length Sholl analyses comparison based on neuron classification and/or genotype. A) Sholl analysis of the total dendritic length in 10µm increments comparing tau and WT neurons. B-F were the same as in A except compared different neuron classifications and/or lineages. B) Comparison of fan and stellate cells. C) Comparison of fan cells by genotype (tau or WT). D) Comparison of stellate cells by genotype (tau or WT). E) Comparison of tau neurons by neuron classification (fan or stellate). F) Comparison of WT neurons by neuron classification (fan or stellate).

Sholl Analysis: Surface Area

As one of the main roles of dendrites is the ability to integrate electrochemical signals from other neurons, dendrite arbors with increased surface area generally have a stronger capability of performing this function due to increased access for other neuronal processes to connect. In this regard, surface area is crucial metric for determining a neuron's interconnectivity to its surrounding environment.

Overall, WT and tau neuron genotypes showed no differences in average surface area of dendrites throughout the Sholl analysis (Fig. 12 A). When also distinguishing by neuron type, however, differences were noted. For example, when comparing WT and tau fan cells, it was noted that tau fan cells had significantly greater surface area in the vicinity of 160-220 μm (Fig. 12 C). On the other hand, while comparing WT and tau stellate cells, no differences in surface area were noted (Fig. 12 D).

When analyzing by neuron type, fan cells were found to have significantly greater surface area between 140-220 μm away from the soma (Fig. 12 B). This pattern was intensified when looking only at tau neurons, where fan cells were found to have statistically significant greater surface at a range of 100-220 μm away from the soma (Fig. 12 E). WT neurons, on the other hand, did not show as strong a trend for one type of neuron having greater surface area, with data only suggesting that stellate cells have a greater average surface area relatively close distance to the soma: 30-40 μm away (Fig. 12 F).

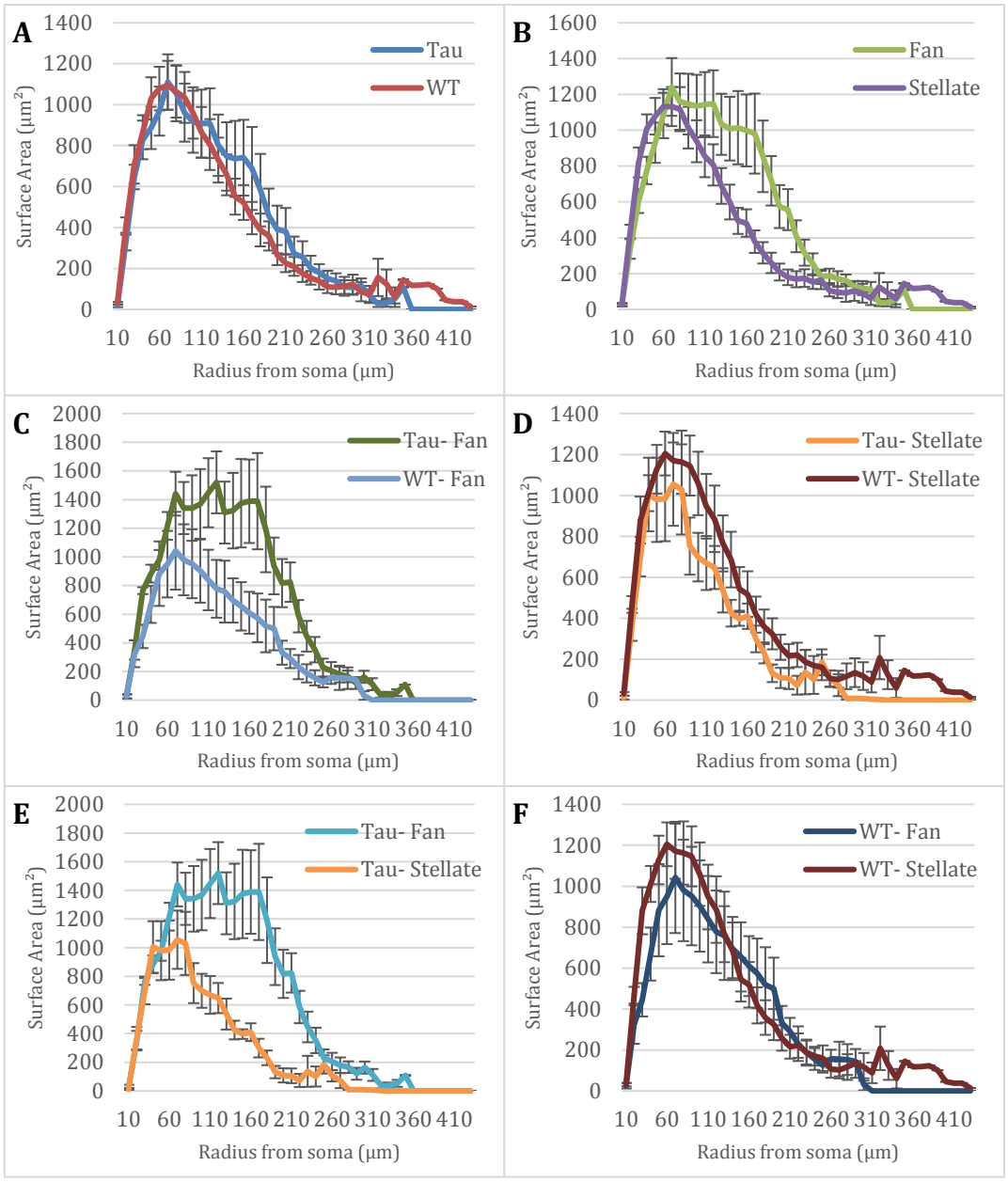

Figure 12. Dendritic surface area Sholl analyses comparison based on neuron classification and/or genotype. A) Sholl analysis of the total surface area in 10µm increments comparing tau and WT neurons. B-F were the same as in A except compared different neuron classifications and/or lineages. B) Comparison of fan and stellate cells. C) Comparison of fan cells by genotype (tau or WT). D) Comparison of stellate cells by genotype (tau or WT). E) Comparison of tau neurons by neuron classification (fan or stellate). F) Comparison of WT neurons by neuron classification (fan or stellate).

Overall Sholl Radius

Lastly, neurons were analyzed to determine average Sholl radius, signifying the greatest extent a dendrite extended from the cell body of the neuron. Interestingly, tau fan cells were found to have the largest Sholl radius of 328.0 ± 22.8 μm (n=5). This was significantly greater than both tau stellate cells (266.0 ± 54.6 μm (n=5), p=0.047) as well as WT fan cells (272.0 ± 27.7 μm (n=5), p=0.009) (Fig. 13).

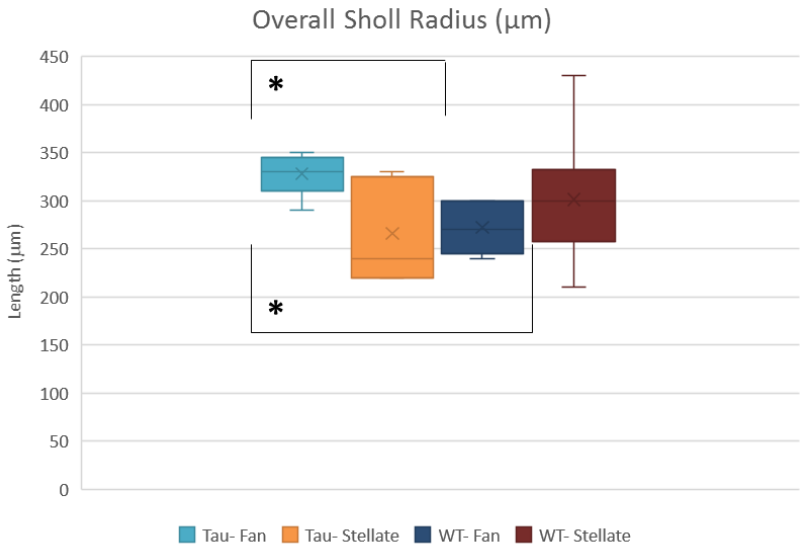

Figure 13. Box and whisker plots of the overall Sholl radius based on neuron classification and genotype. *p<0.05.

3D Convex Hull Analysis

In its simplest understanding, convex hull is an operation utilizing the smallest set of points which when taken together, create a polygon that encompass all other points inside of the shape- in other words it represents the volume of neuropil occupied by the

entirety of the neuron. For the analysis of neurons, the distal most points of the neuron's dendrites act as the points used to create a convex polygon. The significance of this analysis is this shape acts as a representation of the dendritic field for the neuron, allowing for a model representation of the volume and surface area of the neuron.

For both volume and surface area analysis after creating the convex hull, only the comparison of tau fan cells to WT fan cells were found to be statistically significant, with tau fan cells being larger in both categories (volume: p=0.020; surface area: p=0.028) (Fig. 14 A,B). Interestingly, the results in general correspond to the findings from the different categories analyzed during Sholl analysis.

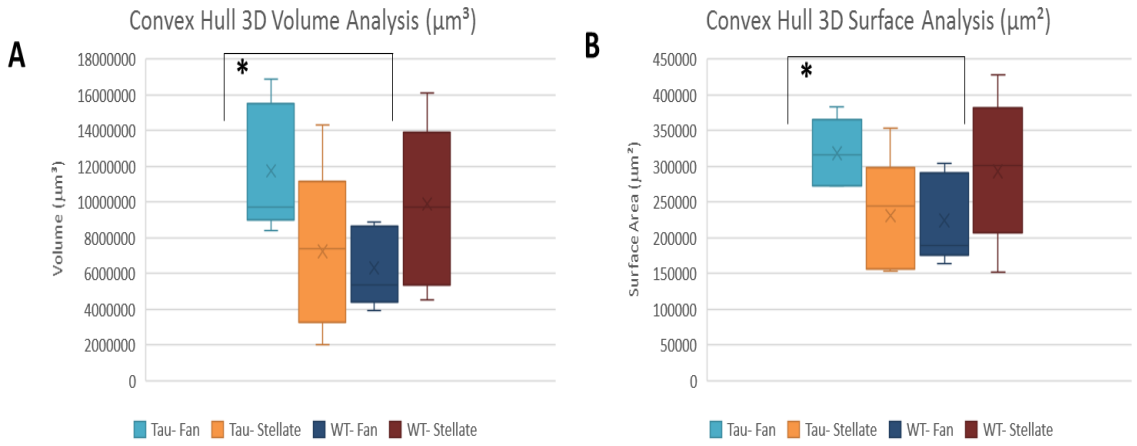

Figure 14. Box and whisker plots of the Convex Hull 3D analysis based on neuron classification and genotype. A) Convex Hull 3D volume analysis based on neuron classification and genotype. B) Convex Hull 3D surface area analysis based on neuron classification and genotype. *p<0.05.

DISCUSSION

The key goal of this study was to determine the effects that tau has on the morphological properties of dendrites of fan and stellate cells in the entorhinal cortex. To do this, the transgenic P301S mouse model was employed, was then compared to a non-transgenic WT mouse genotype. Additionally, cells in the entorhinal cortex were analyzed due to the understanding that this region of the brain being one of the earliest to be affected in the neurodegenerative disease AD, with atrophy noted even in the precursor ailment of MCI (deToldeo-Morrell et al. 2007). Two types of neurons in particular were analyzed to determine differences in response to tauopathies: fan cells and stellate cells.

Interestingly, of the two neuron types studied in depth, very different morphological responses to the presence of mutant tau were observed. Across multiple parameters for measuring dendrites, a common theme found was dendritic regression in stellate cells in tau mutant mice relative to WT. On the other hand, when examining fan cells, it was noted that dendrite complexity actually increased in tau mice in comparison to the WT genotype in some instances. Overall, tau stellate cells were found to have far fewer primary dendrites in comparison to the non-transgenic mouse model ($p=0.004$) (Figure 1 B). When analyzing dendrite complexity, again stellate cells affected by the tauopathy were shown to have fewer nodes and endings when compared to the WT mice (Figure 2 B,D). Fan cells that were exposed to tau, on the other hand, did not demonstrate a decrease in primary dendrites or in complexity. Total dendritic length was another parameter examined, and once again, tau stellate cells exhibited a significant decrease in

length when compare to WT stellate cells (Figure 3 B). It is also interesting to note that tau stellate cells did not differ in mean dendritic length compared to WT stellate cells (Figure 3 D). Taken together with the fact that tau stellate cells had significantly less overall dendritic length compared to WT stellate cells suggests that the atrophy which stellate cells undergo is a reduction in overall number of dendrites rather than shortening of dendrites. The Sholl analysis conducted shows that stellates are negatively affected by tauopathies in the sense that their complexity and dendritic length decreased within dendrites closest to the soma. Conversely, when fan cells were impacted by transgenic tau, their complexity, dendritic length, and surface area actually increased further out from the soma, roughly 130-240 μm from the center. Fan cells were shown to significantly increase in both overall Sholl radius (Figure 7) and increase in three-dimension volume and surface area based on a convex hull analysis when comparing the transgenic tau mouse model to the WT genotype (Figure 8 A,B).

Although many studies have shown that neurodegenerative diseases can have dystrophic effects on neuronal morphology, less is known about the effects tau can have on neuronal structure (Luebke et al. 2010). Previous studies have shown tauopathies resulting from mutant tau negatively impact dendritic arbors by inducing atrophy, causing a decrease in both dendritic length and complexity (Rocher et al. 2010). Some studies have suggested that cells may respond to increased tau by having dendritic proliferation rather than degeneration. Crimins et al. 2012 noted just this when studying frontal cortical slices in layer III for pyramidal neurons from rTg4510 tau mutant mice. At eight months, neurons were labeled as either “intact”—meaning their dendritic morphology did

not vary substantially from the WT genotype, or "atrophic"—meaning that the dendritic morphology was experiencing significant atrophy. Like the fan cells in this study, "intact" transgenic cells in the Crimins et al. 2012 study showed an increase in dendritic length and complexity near the apical arbor, very close to the soma. This somewhat differs in the Sholl analysis conducted for fan cells in this study which showed that compared to WT fan cells, dendritic complexity (based on count of intersections) and dendritic length did not increase until after roughly 100 μm from the soma. Transgenic cells that were considered "atrophic" in the Crimins et al. 2012 study exhibited significant reduction in total dendritic length, similar to how tau stellate cells in this study recorded a loss in dendritic length compared to WT stellate cells. The Crimins et al. 2012 study showed that this group of neurons showed reduction in dendritic length throughout the dendritic arbor; stellate cells in this study, however, showed reduction in dendritic length and complexity only in regions closest to the soma for roughly the first 100 μm. Dickstein et al. 2010 also analyzed pyramidal cells of layer III, this time in the prefrontal cortex. Key findings regarding alterations in dendritic morphology of neurons exposed to tau showed that up to 6 months the only notable difference between htau and WT mice was that htau mice had a shorter basal dendritic length compared to WT mice. At 12 months, despite having a strong presence of hyperphosphorylated tau found in dendrites, there was no noteworthy difference in dendritic length when comparing tau and WT mice. A Sholl analysis conducted in Dickstein et al. 2010 revealed increase in both dendritic length and complexity between 30-120 μm from the soma. In this study, tau fan cells also showed an increase in dendritic length and complexity when a Sholl analysis

was conducted, but tau fan cells in this study only showed increased dendritic length and complexity over WT fan cells further from the soma, at roughly 120-240 μm. That said, it should be noted that Dickstein et al. 2010 utilized non-mutated human tau rather than mutated tau in the mice genotype expressing tau. This is noteworthy as htau may not have the same extent of deleterious effects as found in mutated tau, such as in the P301S mutation which has been found to have a decrease binding affinity for microtubules (Hong et al. 1998).

One important unanswered question in this study is why tau seemed to have a significant but opposite impact on fan and stellate cell dendritic morphology. When analyzing the morphology of fan and stellate cells, one key distinction is the presence of spines. One crucial trait found in stellate cells is their strong propensity for having spines on their dendrites, while fan cell dendrites, contrastingly, are only sparsely populated with spines (Tahvildari and Alonso, 2005). This may be significant as it has been shown that one of the first pathologic loci for tau protein to aggregate once becoming hyperphosphorylated is in spines (Hoover et al. 2010). Once here, damage to the neuron can occur by hyperphosphorylated tau impairing glutamate receptor trafficking and synaptic anchoring, suppressing important synaptic function for the neuron (Hoover et al. 2010). If one cell has a large amount of spines, this may create a fruitful environment for phosphorylated tau to accumulate to a larger degree compared to a neuron which has a lesser spine density. Too great of a spine density may allow tau accumulation to overwhelm the cell through pathologic interactions such as inhibiting axonal transport, potentially creating a stress signal too great for the neuron to respond, thus resulting in a

response of dendritic atrophy. On the other hand, if the stress caused on the neuron from tau accumulation is not as great, the neuron may attempt to alleviate the stressor in a different manner. For example, Crimins et al. 2012 noted that one plausible explanation for the oblique sprouting of dendrites in some neurons impacted by tauopathy could be a result of deafferentation. For example, if a neuron were to lose signaling from one section of a dendrite due to pathologic complications from tau, neural plasticity may allow it to sprout additional dendrites in order to compensate for the initial loss of dendritic signaling to revert back to initial homeostatic conditions (Crimins et al. 2012). Another key difference between fan cell and stellate cells is the way their dendrites distribute. Both cells distribute dendrites into layers I and II, but stellate cells also have dendrites that extend towards layer III (Tahvildari and Alonso, 2005). Wang and Mandelkow, 2016 mention that a plausible mechanism for the spreading of tau pathology involves trans-synaptic spreading. If true, stellate cells would be more vulnerable to this mechanism due to their dendritic arbor being more equally distributed throughout layers I, II, and III, whereas fan cell dendrites branch in a more unidirectional manner through layers I and II towards the pia, subsequently exposing fan cells to less neuronal interactions (Tahvildari and Alonso, 2005).

Overall, this study found a notable response in terms of alterations of dendrite morphology to tau pathogenicity when comparing fan and stellate cells. For future studies, it might be useful to further explore the concept that spine density may be able to promote dendritic atrophy by analyzing spine density in neurons to see if neurons with a high or low density of spines might be resistant to dendritic atrophy commonly seen in

tauopathies. Additionally, attempting to map out an neuronal networks to establish the degree to which neurons are connected might make it feasible to test the concept if trans-synaptic spreading might promote tauopathy and potentially dendritic morphological alterations. Third, although tau is critical in altering dendritic morphology due to its interaction with the neuronal cytoskeleton, stress granules also have been shown to interact with tau, since tauopathies have been shown to increase stress granule density. Therefore, by downregulating an RNA-binding protein such as TIA-1, it would be interesting to see if this altered the ability for stress granule aggregation to occur, and if this might alleviate some of the morphological pathologies affecting dendrite morphology.

Understanding the entorhinal cortex is a crucial stepping stone for better understanding neurodegenerative diseases such as AD, which causes such a high burden on the individuals and families impacted by the disease. It is hopeful that as a better understanding of how tauopathies cause damage to neurons, therapeutic concepts can be designed to treat the earliest regions impacted by AD.

REFERENCES

Agster, Kara L., and Rebecca D. Burwell. "Hippocampal and Subicular Efferents and Afferents of the Perihinal, Postrhinal, and Entorhinal Cortices of the Rat." *Behavioural Brain Research* 254 (2013): 50-64.

Alami, Nael H., Rebecca B. Smith, Monica A. Carrasco, Luis A. Williams, Christina S. Winborn, Steve S. W. Han, Evangelos Kiskinis, et al. "Axonal Transport of TDP-43 mRNA Granules Is Impaired by ALS-Causing Mutations." *Neuron* 81, no. 3 (2014): 536–43.

Alonso, A., and R. Klink. "Differential Electroresponsiveness of Stellate and Pyramidal-like Cells of Medial Entorhinal Cortex Layer II." *Journal of Neurophysiology* 70, no. 1 (1993): 128–43.

Anderson, Lynda A., Richard A. Goodman, Deborah Holtzman, Samuel F. Posner, and Mary E Northridge. "Aging in the United States: Opportunities and Challenges for Public Health." *American Journal of Public Health* 102, no. 3 (2012): 393–95.

Arellano, Jon I., Ruth Benavides-Piccione, Javier DeFelipe, and Rafael Yuste. "Ultrastructure of Dendritic Spines: Correlation Between Synaptic and Spine Morphologies." *Frontiers in Neuroscience* 1, no. 1 (2007): 131–43.

Bielle, F., and S. Garel. "Chapter 25 - Neuronal Migration of Guidepost Cells." In *Cellular Migration and Formation of Neuronal Connections*, edited by John L. R. Rubenstein and Pasko Rakic, 457–79. Oxford: Academic Press, 2013.

Binder, L. I., A. Frankfurter, and L. I. Rebhun. "The Distribution of Tau in the Mammalian Central Nervous System." *The Journal of Cell Biology* 101, no. 4 (1985): 1371–78.

Buchan, J. Ross, and Roy Parker. "Eukaryotic Stress Granules: The Ins and Out of Translation." *Molecular Cell* 36, no. 6 (2009): 932-41.

Buée, L., T. Bussière, V. Buée-Scherrer, A. Delacourte, and P. R. Hof. "Tau Protein Isoforms, Phosphorylation and Role in Neurodegenerative Disorders." *Brain Research. Brain Research Reviews* 33, no. 1 (2000): 95–130.

Burwell, R. D., and K. L. Agster. "3.03 - Anatomy of the Hippocampus and the Declarative Memory System." In *Learning and Memory: A Comprehensive Reference*, edited by John H. Byrne, 47–66. Oxford: Academic Press, 2008.

Canto, Cathrin B., and Menno P. Witter. "Cellular Properties of Principal Neurons in the Rat Entorhinal Cortex. I. The Lateral Entorhinal Cortex." *Hippocampus* 22, no. 6 (2012): 1256–76.

Canto, Cathrin B., Floris G. Wouterlood, and Menno P. Witter. "What Does the Anatomical Organization of the Entorhinal Cortex Tell Us?" *Neural Plasticity* (2008): e381243.

Cohen, Todd J., Jing L. Guo, David E. Hurtado, Linda K. Kwong, Ian P. Mills, John Q. Trojanowski, and Virginia M. Y. Lee. "The Acetylation of Tau Inhibits Its Function and Promotes Pathological Tau Aggregation." *Nature Communications* 2 (2011): 252.

Cook, Casey, Jeannette N. Stankowski, Yari Carlomagno, Caroline Stetler, and Leonard Petrucelli. "Acetylation: A New Key to Unlock Tau's Role in Neurodegeneration." *Alzheimer's Research & Therapy* 6 (2014): 29.

Craig, Sarah, and Sean Commins. "The Subiculum to Entorhinal Cortex Projection Is Capable of Sustaining Both Short- and Long-Term Plastic Changes." *Behavioural Brain Research*, The Mammalian Subiculum: Contrasting and complementary in vivo and in vitro approaches to subicular function, 174, no. 2 (2006): 281–88.

Crimins, Johanna L., Anne B. Rocher, and Jennifer I. Luebke. "Electrophysiological Changes Precede Morphological Changes to Frontal Cortical Pyramidal Neurons in the rTg4510 Mouse Model of Progressive Tauopathy." *Acta Neuropathologica* 124, no. 6 (2012): 777–95.

DeVos, Sarah L., Rebecca L. Miller, Kathleen M. Schoch, Brandon B. Holmes, Carey S. Kebodeaux, Amy J. Wegener, Guo Chen, et al. "Tau Reduction Prevents Neuronal Loss and Reverses Pathological Tau Deposition and Seeding in Mice with Tauopathy." *Science Translational Medicine* 9, no. 374 (2017): eaag0481.

Dharmarajan, T.S., and Srinivas G. Gunturu. "Alzheimer's Disease: A Healthcare Burden of Epidemic Proportion." *American Health & Drug Benefits* 2, no. 1 (2009): 39–47.

Dickstein, Dara L., Hannah Brautigam, Steven D. Stockton, James Schmeidler, and Patrick R. Hof. "Changes in Dendritic Complexity and Spine Morphology in Transgenic Mice Expressing Human Wild-Type Tau." *Brain Structure & Function* 214, no. 2–3 (2010): 161–79.

Ding, Qunxing, William R. Markesbery, Qinghua Chen, Feng Li, and Jeffrey N. Keller. "Ribosome Dysfunction Is an Early Event in Alzheimer's Disease." *The Journal of Neuroscience: The Official Journal of the Society for Neuroscience* 25, no. 40 (2005): 9171–75.

Ewers, Michael, Cathal Walsh, John Q. Trojanowski, Leslie M. Shaw, Ronald C. Petersen, Clifford R. Jack, Howard H. Feldman, et al. "Prediction of Conversion from Mild Cognitive Impairment to Alzheimer's Disease Dementia Based upon Biomarkers and Neuropsychological Test Performance." *Neurobiology of Aging* 33, no. 7 (2012): 1203–1214.e2.

Geldmacher, David S. "Cost-Effective Recognition and Diagnosis of Dementia." *Seminars in Neurology* 22, no. 1 (2002): 63–70.

Glodzik, Lidia, Susan de Santi, Wai Hon Tsui, Lisa Mosconi, Raymond Zinkowski, Elizabeth Pirraglia, Hui Yu Wang, et al. "Phosphorylated Tau 231, Memory Decline and Medial Temporal Atrophy in Normal Elders." *Neurobiology of Aging* 32, no. 12 (2011): 2131–41.

Gómez-Isla, Teresa, Joseph L. Price, Daniel W. McKeel Jr, John C. Morris, John H. Growdon, and Bradley T. Hyman. "Profound Loss of Layer II Entorhinal Cortex Neurons Occurs in Very Mild Alzheimer's Disease." *Journal of Neuroscience* 16, no. 14 (1996): 4491–4500.

Gómez-Río, Manuel, Manuel Moreno Caballero, Juan Manuel Górriz Sáez, and Adolfo Mínguez-Castellanos. "Diagnosis of Neurodegenerative Diseases: The Clinical Approach." *Current Alzheimer Research* 13, no. 5 (2016): 469–74.

Hebert, Liesi E., Paul A. Scherr, Julia L. Bienias, David A. Bennett, and Denis A. Evans. "Alzheimer Disease in the US Population: Prevalence Estimates Using the 2000 Census." *Archives of Neurology* 60, no. 8 (2003): 1119–22.

Hoffmann, Nadine A, Mario M Dorostkar, Sonja Blumenstock, Michel Goedert, and Jochen Herms. "Impaired Plasticity of Cortical Dendritic Spines in P301S Tau Transgenic Mice." *Acta Neuropathologica Communications* 1 (2013): 82.

Hong, Ming, Victoria Zhukareva, Vanessa Vogelsberg-Ragaglia, Zbigniew Wszolek, Lee Reed, Bruce I. Miller, Dan H. Geschwind, et al. "Mutation-Specific Functional Impairments in Distinct Tau Isoforms of Hereditary FTDP-17." *Science* 282, no. 5395 (1998): 1914–17.

Hoover, Brian R., Miranda N. Reed, Jianjun Su, Rachel D. Penrod, Linda A. Kotilinek, Marianne K. Grant, Rose Pitstick, et al. "Tau Mislocalization to Dendritic Spines Mediates Synaptic Dysfunction Independently of Neurodegeneration." *Neuron* 68, no. 6 (2010): 1067–81.

Jaworski, J., M. Psujek, and H. Bartosik-Psujek. "Total-Tau and Phospho-tau(181Thr) in Cerebrospinal Fluid of Neurologically Intact Population Increase with Age." *Folia Biologica* 55, no. 4 (2009): 126–31.

Jin, Ming, Nina Shepardson, Ting Yang, Gang Chen, Dominic Walsh, and Dennis J. Selkoe. "Soluble Amyloid Beta-Protein Dimers Isolated from Alzheimer Cortex Directly Induce Tau Hyperphosphorylation and Neuritic Degeneration." *Proceedings of the National Academy of Sciences of the United States of America* 108, no. 14 (2011): 5819–24.

Kasai, Haruo, Masahiro Fukuda, Satoshi Watanabe, Akiko Hayashi-Takagi, and Jun Noguchi. "Structural Dynamics of Dendritic Spines in Memory and Cognition." *Trends in Neurosciences* 33, no. 3 (2010): 121–29.

Kedersha, N. L., M. Gupta, W. Li, I. Miller, and P. Anderson. "RNA-Binding Proteins TIA-1 and TIAR Link the Phosphorylation of eIF-2 Alpha to the Assembly of Mammalian Stress Granules." *The Journal of Cell Biology* 147, no. 7 (1999): 1431–42.

Kedersha, Nancy, and Paul Anderson. "Mammalian Stress Granules and Processing Bodies." edited by BT - Methods in Enzymology, 431:61–81. Translation Initiation: Cell Biology, High-Throughput Methods, and Chemical-Based Approaches. Academic Press, 2007.

Khan, Usman A., Li Liu, Frank A. Provenzano, Diego E. Berman, Caterina P. Profaci, Richard Sloan, Richard Mayeux, Karen E. Duff, and Scott A. Small. "Molecular Drivers and Cortical Spread of Lateral Entorhinal Cortex Dysfunction in Preclinical Alzheimer's Disease." *Nature Neuroscience* 17, no. 2 (2014): 304–11.

Klein, Alexandra S., José R. Donoso, Richard Kempter, Dietmar Schmitz, and Prateep Beed. "Early Cortical Changes in Gamma Oscillations in Alzheimer's Disease." *Frontiers in Systems Neuroscience* 10: 83 (2016).

Knierim, James J., Inah Lee, and Eric L. Hargreaves. "Hippocampal Place Cells: Parallel Input Streams, Subregional Processing, and Implications for Episodic Memory." *Hippocampus* 16, no. 9 (2006): 755–64.

Knowles, R. B., J. H. Sabry, M. E. Martone, T. J. Deerinck, M. H. Ellisman, G. J. Bassell, and K. S. Kosik. “Translocation of RNA Granules in Living Neurons.” *The Journal of Neuroscience: The Official Journal of the Society for Neuroscience* 16, no. 24 (1996): 7812–20.

Kordower, J. H., Y. Chu, G. T. Stebbins, S. T. DeKosky, E. J. Cochran, D. Bennett, and E. J. Mufson. “Loss and Atrophy of Layer II Entorhinal Cortex Neurons in Elderly People with Mild Cognitive Impairment.” *Annals of Neurology* 49, no. 2 (2001): 202–13.

Lasagna-Reeves, Cristian A., Diana L. Castillo-Carranza, Urmi Sengupta, Audra L. Clos, George R. Jackson, and Rakez Kayed. “Tau Oligomers Impair Memory and Induce Synaptic and Mitochondrial Dysfunction in Wild-Type Mice.” *Molecular Neurodegeneration* 6 (2011): 39.

Lee, Gloria, and Chad J. Leugers. “Tau and Tauopathies.” *Progress in Molecular Biology and Translational Science* 107 (2012): 263–93.

Lee, V. M., M. Goedert, and J. Q. Trojanowski. “Neurodegenerative Tauopathies.” *Annual Review of Neuroscience* 24 (2001): 1121–59.

Li, G., and S. J. Pleasure. “Chapter 18 - Migration in the Hippocampus.” In *Cellular Migration and Formation of Neuronal Connections*, edited by John L. R. Rubenstein and Pasko Rakic, 331–43. Oxford: Academic Press, 2013.

Liu-Yesucevitz, Liqun, Gary J. Bassell, Aaron D. Gitler, Anne C. Hart, Eric Klann, Joel D. Richter, Stephen T. Warren, and Benjamin Wolozin. “Local RNA Translation at the Synapse and in Disease.” *The Journal of Neuroscience: The Official Journal of the Society for Neuroscience* 31, no. 45 (2011): 16086–93.

Liu-Yesucevitz, Liqun, Aylin Bilgutay, Yong-Jie Zhang, Tara Vanderweyde, Tara Vanderwyde, Allison Citro, Tapan Mehta, et al. “Tar DNA Binding Protein-43 (TDP-43) Associates with Stress Granules: Analysis of Cultured Cells and Pathological Brain Tissue.” *PloS One* 5, no. 10 (2010): e13250.

Luebke, Jennifer I., Christina M. Weaver, Anne B. Rocher, Alfredo Rodriguez, Johanna L. Crimins, Dara L. Dickstein, Susan L. Wearne, and Patrick R. Hof. “Dendritic Vulnerability in Neurodegenerative Disease: Insights from Analyses of Cortical Pyramidal Neurons in Transgenic Mouse Models.” *Brain Structure & Function* 214, no. 2–3 (2010): 181–99.

Marcantoni, Andrea, Elisabeth F. Raymond, Emilio Carbone, and Hélène Marie. “Firing Properties of Entorhinal Cortex Neurons and Early Alterations in an Alzheimer’s Disease Transgenic Model.” *Pflügers Archiv - European Journal of Physiology* 466, no. 7 (2014): 1437–50.

Marciniak, Stefan J., Lidia Garcia-Bonilla, Junjie Hu, Heather P. Harding, and David Ron. “Activation-Dependent Substrate Recruitment by the Eukaryotic Translation Initiation Factor 2 Kinase PERK.” *The Journal of Cell Biology* 172, no. 2 (2006): 201–9.

Meier, Shelby, Michelle Bell, Danielle N. Lyons, Jennifer Rodriguez-Rivera, Alexandria Ingram, Sarah N. Fontaine, Elizabeth Mechas, et al. “Pathological Tau Promotes Neuronal Damage by Impairing Ribosomal Function and Decreasing Protein Synthesis.” *The Journal of Neuroscience* 36, no. 3 (2016): 1001–7.

Min, Sang-Won, Seo-Hyun Cho, Yungui Zhou, Sebastian Schroeder, Vahram Haroutunian, William W. Seeley, Eric J. Huang, et al. “Acetylation of Tau Inhibits Its Degradation and Contributes to Tauopathy.” *Neuron* 67, no. 6 (2010): 953–66.

Morrell, Leyla deToledo-, Travis R. Stoub, and Changsheng Wang. “Hippocampal Atrophy and Disconnection in Incipient and Mild Alzheimer’s Disease.” In *Progress in Brain Research*, edited by Helen E. Scharfman, 163:741–823. The Dentate Gyrus: A Comprehensive Guide to Structure, Function, and Clinical Implications. Elsevier, 2007.

Parron, Carole, Bruno Poucet, and Etienne Save. “Entorhinal Cortex Lesions Impair the Use of Distal but Not Proximal Landmarks during Place Navigation in the Rat.” *Behavioural Brain Research* 154, no. 2 (2004): 345–52.

Phillips, Kristine, Nancy Kedersha, Lily Shen, Perry J. Blackshear, and Paul Anderson. “Arthritis Suppressor Genes TIA-1 and TTP Dampen the Expression of Tumor Necrosis Factor A, Cyclooxygenase 2, and Inflammatory Arthritis.” *Proceedings of the National Academy of Sciences of the United States of America* 101, no. 7 (2004): 2011–16.

Ricobaraza, Ana, Mar Cuadrado-Tejedor, Sonia Marco, Isabel Pérez-Otaño, and Ana García-Osta. “Phenylbutyrate Rescues Dendritic Spine Loss Associated with Memory Deficits in a Mouse Model of Alzheimer Disease.” *Hippocampus* 22, no. 5 (2012): 1040–50.

Ritchie, Karen, Sylvaine Artero, and Jacques Touchon. “Classification Criteria for Mild Cognitive Impairment A Population-Based Validation Study.” *Neurology* 56, no. 1 (2001): 37–42.

Rizzu, P., J. C. Van Swieten, M. Joosse, M. Hasegawa, M. Stevens, A. Tibben, M. F. Niermeijer, et al. “High Prevalence of Mutations in the Microtubule-Associated Protein Tau in a Population Study of Frontotemporal Dementia in the Netherlands.” *American Journal of Human Genetics* 64, no. 2 (1999): 414–21.

Rocher, A. B., J. L. Crimins, J. M. Amatrudo, M. S. Kinson, M. A. Todd-Brown, J. Lewis, and J. I. Luebke. “Structural and Functional Changes in Tau Mutant Mice Neurons Are Not Linked to the Presence of NFTs.” *Experimental Neurology* 223, no. 2 (2010): 385–93.

Romito-DiGiacomo, Rita R., Harry Menegay, Samantha A. Cicero, and Karl Herrup. “Effects of Alzheimer’s Disease on Different Cortical Layers: The Role of Intrinsic Differences in Aβ Susceptibility.” *Journal of Neuroscience* 27, no. 32 (2007): 8496–8504.

Roy, Subhojit, Bin Zhang, Virginia M.-Y. Lee, and John Q. Trojanowski. “Axonal Transport Defects: A Common Theme in Neurodegenerative Diseases.” *Acta Neuropathologica* 109, no. 1 (2005): 5–13.

SantaCruz, K., J. Lewis, T. Spires, J. Paulson, L. Kotilinek, M. Ingelsson, A. Guimaraes, et al. “Tau Suppression in a Neurodegenerative Mouse Model Improves Memory Function.” *Science (New York, N.Y.)* 309, no. 5733 (2005): 476–81.

Schulz, Richard, Kathleen A. McGinnis, Song Zhang, Lynn M. Martire, Randy S. Hebert, Scott R. Beach, Bozena Zdaniuk, Sara J. Czaja, and Steven H. Belle. “Dementia Patient Suffering and Caregiver Depression.” *Alzheimer Disease and Associated Disorders* 22, no. 2 (2008): 170–76.

Selkoe, Dennis J. “Alzheimer’s Disease: Genes, Proteins, and Therapy.” *Physiological Reviews* 81, no. 2 (2001): 741–66.

Spillantini, Maria Grazia, and Michel Goedert. “Tau Pathology and Neurodegeneration.” *The Lancet. Neurology* 12, no. 6 (2013): 609–22.

Stamer, K., R. Vogel, E. Thies, E. Mandelkow, and E.-M. Mandelkow. “Tau Blocks Traffic of Organelles, Neurofilaments, and APP Vesicles in Neurons and Enhances Oxidative Stress.” *The Journal of Cell Biology* 156, no. 6 (2002): 1051–63.

Tagawa, Kazuhiko, Hidenori Homma, Ayumu Saito, Kyota Fujita, Xigui Chen, Seiya Imoto, Tsutomu Oka, et al. “Comprehensive Phosphoproteome Analysis Unravels the Core Signaling Network That Initiates the Earliest Synapse Pathology in Preclinical Alzheimer’s Disease Brain.” *Human Molecular Genetics* 24, no. 2 (2015): 540–58.

Tahvildari, Babak, and Angel Alonso. “Morphological and Electrophysiological Properties of Lateral Entorhinal Cortex Layers II and III Principal Neurons.” *The Journal of Comparative Neurology* 491, no. 2 (2005): 123–40.

Takeuchi, Hiroki, Michiyo Iba, Haruhisa Inoue, Makoto Higuchi, Keizo Takao, Kayoko Tsukita, Yoshiko Karatsu, et al. “P301S Mutant Human Tau Transgenic Mice Manifest Early Symptoms of Human Tauopathies with Dementia and Altered Sensorimotor Gating.” *PLOS ONE* 6, no. 6 (2011): e21050.

Testa, Ilaria, Nicolai T. Urban, Stefan Jakobs, Christian Eggeling, Katrin I. Willig, and Stefan W. Hell. “Nanoscopy of Living Brain Slices with Low Light Levels.” *Neuron* 75, no. 6 (2012): 992–1000.

Vanderweyde, Tara, Katie Youmans, Liqun Liu-Yesucevitz, and Benjamin Wolozin. “Role of Stress Granules and RNA-Binding Proteins in Neurodegeneration: A Mini-Review.” *Gerontology* 59, no. 6 (2013): 524–33.

Vanderweyde, Tara, Haung Yu, Megan Varnum, Liqun Liu-Yesucevitz, Allison Citro, Tsuneya Ikezu, Karen Duff, and Benjamin Wolozin. “Contrasting Pathology of the Stress Granule Proteins TIA-1 and G3BP in Tauopathies.” *The Journal of Neuroscience* 32, no. 24 (2012): 8270–83.

Vossel, Keith A., Kai Zhang, Jens Brodbeck, Aaron C. Daub, Punita Sharma, Steven Finkbeiner, Bianxiao Cui, and Lennart Mucke. “Tau Reduction Prevents Abeta-Induced Defects in Axonal Transport.” *Science (New York, N.Y.)* 330, no. 6001 (2010): 198.

Wang, Yipeng, and Eckhard Mandelkow. “Tau in Physiology and Pathology.” *Nature Reviews Neuroscience* 17, no. 1 (2016): 22–35.

Wesson, Daniel W., Efrat Levy, Ralph A. Nixon, and Donald A. Wilson. “Olfactory Dysfunction Correlates with Amyloid-β Burden in an Alzheimer’s Disease Mouse Model.” *The Journal of Neuroscience : The Official Journal of the Society for Neuroscience* 30, no. 2 (2010): 505–14.

Wilson, R. C., and O. Steward. “Polysynaptic Activation of the Dentate Gyrus of the Hippocampal Formation: An Olfactory Input via the Lateral Entorhinal Cortex.” *Experimental Brain Research* 33, no. 3–4 (1978): 523–34.

Wolozin, Benjamin. “Regulated Protein Aggregation: Stress Granules and Neurodegeneration.” *Molecular Neurodegeneration* 7 (2012): 56.

Wolozin, Benjamin. “Physiological Protein Aggregation Run Amuck: Stress Granules and the Genesis of Neurodegenerative Disease.” *Discovery Medicine* 17, no. 91 (2014): 47–52.

Xu, Hong, Thomas W. Rösler, Thomas Carlsson, Anderson de Andrade, Julius Bruch, Matthias Höllerhage, Wolfgang H. Oertel, and Günter U. Höglinger. “Memory Deficits Correlate with Tau and Spine Pathology in P301S MAPT Transgenic Mice.” *Neuropathology and Applied Neurobiology* 40, no. 7 (2014): 833–43.

Yoo, Seung-Woo, and Inah Lee. “Functional Double Dissociation within the Entorhinal Cortex for Visual Scene-Dependent Choice Behavior.” *eLife* 6 (2017).

Yoshiyama, Yasumasa, Makoto Higuchi, Bin Zhang, Shu-Ming Huang, Nobuhisa Iwata, Takaomi C. Saido, Jun Maeda, Tetsuya Suhara, John Q. Trojanowski, and Virginia M. -Y. Lee. “Synapse Loss and Microglial Activation Precede Tangles in a P301S Tauopathy Mouse Model.” *Neuron* 53, no. 3 (2007): 337–51.

Zhang, Bin, Makoto Higuchi, Yasumasa Yoshiyama, Takeshi Ishihara, Mark S. Forman, Dan Martinez, Sonali Joyce, John Q. Trojanowski, and Virginia M.-Y. Lee. “Retarded Axonal Transport of R406W Mutant Tau in Transgenic Mice with a Neurodegenerative Tauopathy.” *Journal of Neuroscience* 24, no. 19 (2004): 4657–67.

Zhang, Cheng-Cheng, Ang Xing, Meng-Shan Tan, Lan Tan, and Jin-Tai Yu. “The Role of MAPT in Neurodegenerative Diseases: Genetics, Mechanisms and Therapy.” *Molecular Neurobiology* 53, no. 7 (2016): 4893–4904.

CURRICULUM VITAE

MICHAEL FOWLER

Year of Birth: 1989
549 Live Oak Way, Dublin, GA 31021
76 Egmont St., Brookline, MA 02246
Email: fowlerm7@bu.edu

Education:

Boston University School of Medicine, Boston, MA
Candidate for Master of Science in Medical Sciences, May, 2017

Marquette University
Bachelor of Science, August 2011

Research Experience:

Student Research Assistant for Neuroanatomy Lab
August 2016-March 2017

o *Purpose*: To assess neurodegenerative tauopathies in the entorhinal cortex. By utilizing laser-scanning confocal microscopy, dendritic morphology was analyzed to determine effects from P301S transgenic model. Results suggested difference in morphological results when comparing fan and stellate cells, with stellate cells showing dendritic atrophy, while fan cells portrayed dendritic growth and enhanced complexity.

o *Specific Tasks*:

- Collected images of neurons using laser-scanning confocal microscope
- Reconstructed neuron images using NeuroLucida 360.
- Analyzed dendritic parameters using NeuroLucida Explorer.
- Analyzed and presented data in thesis format

Student Research Assistant for Salamander Ecotoxin Project
January 2013-July 2013

o *Purpose*: To assess common pesticide and herbicide levels in local streams in the metro Atlanta region as well as salamander population data regarding both species abundance and species richness. It is hoped that this data will help determine if salamander population measurements in the metro Atlanta region can be correlated with levels of specific pesticides and/or herbicides in the region.

o *Specific Tasks*:

- Assist in collecting knowledge on atrazine including legislation, physical characteristics, intended uses, environmental impacts, and academic literature regarding its impact on amphibians.
- Assist team in capture, measurement, and identification of different stream salamanders for research purposes.

Undergraduate Research Associate for the Biomedical Engineering ALS Project: Dynamic Meta-Analysis of the G93A Mouse Model of ALS
January 2013-April 2013

o *Purpose*: To review academic literature in order to establish a database regarding treatment and corresponding results/symptoms for G93A ALS Mice. It is hoped that through establishment of this database, patterns regarding treatment options and symptomatic responses may identify treatment combinations that yield synergetic effects.

o *Specific Tasks*:

- Review academic articles regarding G93A modeled ALS mice and classify the data collected into correct corresponding input values.

Undergraduate Research Associate for the Biomedical Engineering ALS Project: Clinical ALS Research at Emory University
May 2013-July 2013

o *Purpose:* To review data from patient chart histories who were at the ALS Clinic at Emory University. By collecting these data points, it is hoped that they can be utilized for identifying clinical predictors that can assist in understanding disease prognosis and assist medical professionals in making time-sensitive treatment decisions.

o *Specific Tasks:*

- Review medical records of different patients, inputting both quantitative and qualitative data points found in the patient records as a means to track the progression of the disease.

Medically Relevant Experiences:

Native American Health Center, Program Assistant
August 2014—August 2015

Work at a school-based health clinic that works to provide students and their families access to medical and dental healthcare, health education, and assistance in enrollment in public benefits programs for healthcare. Primary role is to help with the day-to-day functions that the clinic provides including administration of first aid, checking-in of

patients during clinic days, work as the medical assistant on clinic days, and assist in health education courses provided at the clinic.
Also responsible for collecting, analyzing, and reporting data for both services provided at the specific health clinic I work at as well as for projects being conducted throughout multiple or all school-based health clinics at Native American Health Center.